149

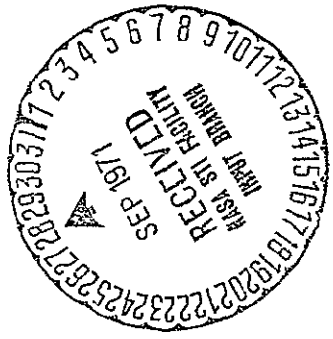

JET PROPULSION LABORATORY
CALIFORNIA INSTITUTE OF TECHNOLOGY
PASADENA CALIFORNIA

Report No TE5107-145-71

FINAL REPORT
DESIGN STUDY OF A HIGH FUEL FRACTION, EXTERNALLY-FUELED THERMIONIC DIODE SUITABLE FOR IN-PILE TESTING

by

Donald M Ernst

May 1971

Prepared for

Jet Propulsion Laboratory

Contract No 952469

Prepared by

Thermo Electron Corporation
85 First Avenue
Waltham, Massachusetts 02154

NOTICE

This report contains information prepared by Thermo Electron Corporation under JPL subcontract Its content is not necessarily endorsed by the Jet Propulsion Laboratory, California Institute of Technology, or the National Aeronautics and Space Administration

TABLE OF CONTENTS

TABLE OF CONTENTS (continued)

LIST OF ILLUSTRATIONS

LIST OF ILLUSTRATIONS (continued)

ACKNOWLEDGEMENT

This report was prepared by Thermo Electron Corporation for the Jet Propulsion Laboratory's Thermionic Reactor Systems Project under the direction of Jack F Mondt The designated JPL technical representative was M Peelgren Responsibility at Thermo Electron belonged to the Direct Conversion and Electronics Group, under the direction of Arvin Smith The Nuclear Thermionics Department, under the direction of John Dunlay, carried out the program Project responsibility was assigned to Donald M Ernst, who supervised and coordinated all aspects of the program

GLOSSARY

dR	=	Radial displacement, inches
W	=	Load, lbs
R	=	Radius, inches
E	=	Modulus of elasticity, lbs/square inch
I	=	Moment of inertia, inches^4
c	=	Distance over which forces act causing moment
M	=	Moment, inch-pounds
2θ	=	Angular displacement between load points, radians
σ	=	Stress, lbs/in^2
ϵ	=	Strain, inches/inch
L	=	Length of web, 10 inches
t	=	Thickness of web or cylinder, inches
ℓ	=	Width of web, inches
R_2	=	Inner radius of outer can, 1 21 inches
R_1	=	Outer radius of emitter, 0 670 inches
α_n	=	Coefficient of thermal expansion of material at T_n
ΔT_n	=	Change from room temperature of material to T_n
$\overline{\alpha_{12}\Delta T_{12}}$	=	Average values between two tempertures $= \dfrac{\alpha_1 \Delta T_1 + \alpha_2 \Delta T_2}{2}$
$\sigma_{y\ s}$	=	0 02% offset yield strength
m	=	$\dfrac{1}{\nu}$
ν	=	Poisson Ratio (for tungsten = 28)

I INTRODUCTION

Under Contract No 952469 with the Jet Propulsion Laboratory, Thermo Electron designed, fabricated, and performance tested an unfueled, externally-configured thermionic diode. This diode was delivered to JPL in July 1970 for additional testing and evaluation.

The contract provided for additional work on the engineering design of a high fuel fraction diode for in-pile testing. Concurrent with this design effort was an investigation of the fabrication of critical components in the diode design and an evaluation of these components under typical thermal and stress operating conditions.

This report summarizes in detail the results of the design study, including the critical component investigations. The preliminary design study showed, by thermal stress analysis, that with all other conditions equal, the stress considerations favor the unbonded emitter-fuel structure concept: there is no permanent deformation of any of the components of the unbonded emitter-fuel structure, and the residual stress at room temperature after numerous thermal cycles is reduced to a minimum. However, since the all-bonded emitter-fuel structure has not only the advantage of lower ohmic losses, but also the capability of being tested with fuel in place, and since it has fewer components and is a two-material (rather than a four-material) system, three representative sample all-bonded emitter-fuel structures were fabricated and tested to investigate their structural integrity experimentally.

Preliminary test results indicate that an all vapor-deposited fluoride tungsten, all-bonded structure appears to be satisfactory from

fabrication and operational points of view However, additional thermal testing of an all-bonded structure with representative fuel end closures should be performed to explore the effects of the non-flexible members After successful operation of an all-bonded structure, including fuel closure end caps, Thermo Electron recommends pursuing the all-bonded design with the fabrication, testing, and in-pile testing of a high fuel fraction thermionic diode

In Section II, the technical background upon which the study was made is presented, followed by the detailed description of the fueled diode design in Section III Section IV details the criteria upon which the design was based, the thermal analysis, and the results of the component development and thermal testing Stress analysis data are presented in Section V The conclusions and recommendations (Section VII) are based on the results of testing (Section VI) and their effects on the diode design The appendix contains pertinent design calculations

II TECHNICAL BACKGROUND

The design of the fueled externally configured diode which is presented here was achieved by the integration of JPL's fuel element concept with the design of the unfueled diode as delivered on this contract

A FUEL ELEMENT CONCEPT

The conceptual design of a high fuel volume fraction-external fuel thermionic fuel element is shown in Figure 1 This concept utilizes a thin wall fuel-emitter structure to achieve a high fuel volume fraction A cross section of this structure is included in Figure 1 The structure consists of the inner tungsten emitter cylinder, the outer concentric fuel containment cylinder, and interconnecting webs The axially positioned webs aid in heat transfer between the nuclear fuel and the emitter and also contribute to the axial electrical path on the emitter side of the diode Nuclear fuel (e g , UO_2) is located in the segmented volumes defined by the webs and the concentric cylinders

The niobium-1% zirconium collector is located within and is concentric to the emitter Cooling of the collector is provided by direct forced flow of liquid metal (NaK) through the center of the collector The liquid metal contributes significantly to the electrical path on the collector side of the diode

The ends of the fuel element concept include closures for the diode and fuel containment, ceramic-to-metal seals for electrical insulation between the emitter and collector, and expansion members

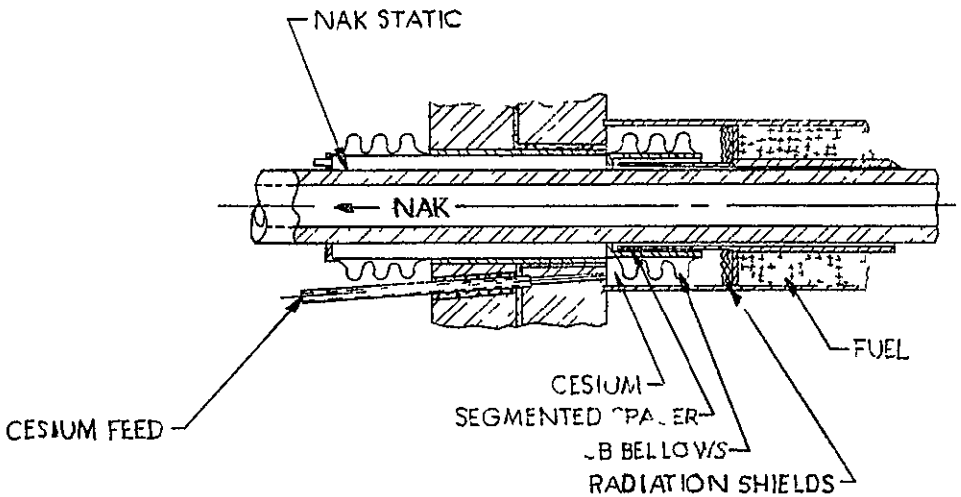

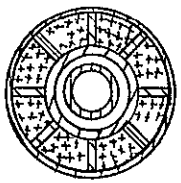

Figure 1. Reactor Fuel Element Concept

to accommodate thermal expansion differences between components Electrical power is removed at both ends of the fuel element to minimize internal electrical losses The ceramic-to-metal seals are located external to the fueled region of the fuel element to minimize the effects of radiation damage to ceramic materials

B UNFUELED DIODE DESIGN

The diode as delivered is shown in Figure 2 The CVD fluoride tungsten emitter has an inner diameter of 0 450 inch, an outer diameter of 0 800 inch, and is 10 inches long The active electrode surface of the emitter is the mandrel side, which was chemically etched for 15 minutes with equal volumes of 5% sodium hydroxide and saturated potassium ferracyanide The 0 040 inch thick tungsten sleeves on each end are integral to the emitter and are attached to niobium flanges which serve as electrical leads and mechanical supports

The niobium-1% zirconium collector has an outer diameter of 0 430 inch and an inner diameter of 0 250 inch The active electrode surface is a few microns of molybdenum, condensed on the collector from a molybdenum filament The collector has three yttria-stabilized zirconia inserts, held in place with rhenium wires, to reduce the possibility of emitter-collector contact due to thermally induced stresses

The collector flanges support the niobium-alumina lead through niobium bellows assemblies, which in turn are welded to the emitter flanges Enclosed within the emitter flanges is an alumina ring, which aids in maintaining the interelectrode spacing Brazed to each collector flange is a copper "bird cage" which serves as a flexible

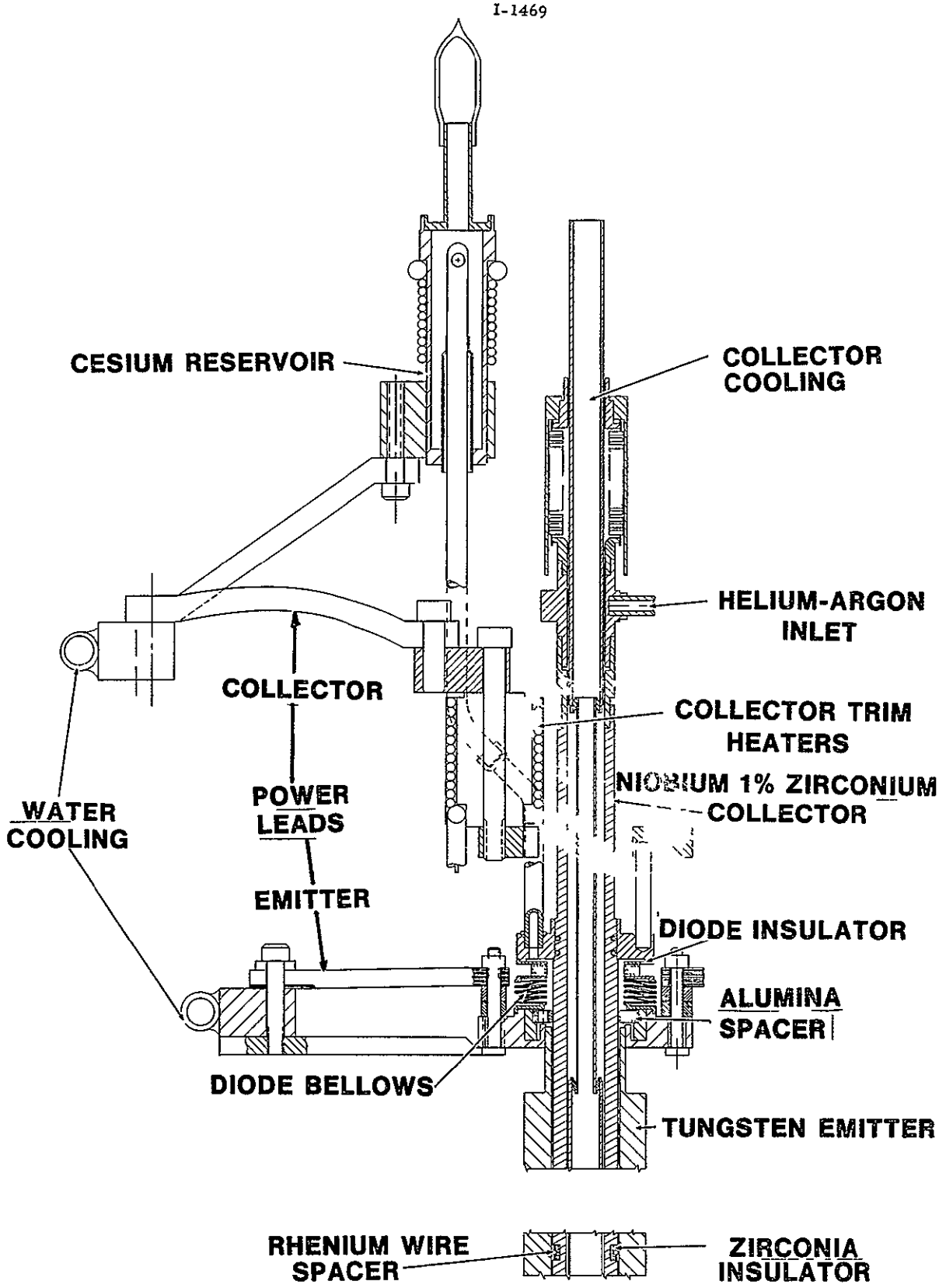

Figure 2 Externally Configured Unfueled Diode

electrical lead and mechanical support The collector is cooled by water through a variable conductance helium-argon 0 007 inch gap Trim heaters are attached to the collector leads to compensate for heat losses down the leads

III FUELED DIODE DESCRIPTION

The overall detailed fueled diode description is presented here, along with the changes necessary for incorporating the diode design into a suitable in-pile capsule for testing at the Battelle Research Reactor

A DIODE DESCRIPTION

The proposed full length fueled diode is seen in Figure 3 The tungsten emitter, which has an inner diameter of 0 550 inch and an outer diameter of 0 670 inch and is 10 inches long, has 16 equally-spaced, 0 030 inch wide longitudinal webs attached to it These webs provide additional radial thermal conductivity, which aids the nuclear fuel in heating the emitter, and additional axial electrical conductivity, which aids in the removal of the generated current The available fuel volume is 55 7%, the fuel is UO_2 The outer tungsten-5% rhenium fuel enclosure, which has an outer diameter of 1 300 inches and a 0 025 inch thick wall, is not bonded to the webs, and is attached only to the emitter sleeves through a flexible member Between the fuel and the outer fuel containers and end enclosures are a few layers of tungsten radiation shields, which aid in reducing both the heat loss from the fuel and the operating temperature of the outer fuel enclosure

The flexible end enclosures on the outer fuel containment are made from the ductile tungsten-25% rhenium and molybdenum-50% rhenium alloys, the tungsten alloy for the higher temperature and the molybdenum alloy for the lower temperatures The molybdenum-50% rhenium is joined directly to the 0 040 inch thick tungsten sleeves which are integral to the emitter Pressure-bonded to the molybdenum-50%

rhenium portion of the fuel end closure is a niobium flange which includes the fission gas vent The flange also allows the joining of the fuel-emitter assembly to the collector assembly through a niobium-niobium joint

The niobium-1% zirconium collector, which has an inner diameter of 0 300 inch and an outer diameter of 0 530 inch, is cooled with the liquid metal (NaK) There are five niobium-alumina cermets pressure-bonded to the collector, they are grooved to accept the rhenium wires utilized to offset possible emitter-collector contact resulting from thermally induced stresses On one end, the collector is joined to the emitter through a niobium-alumina insulator assembly On the other end, there is a niobium-1% zirconium bellows assembly between the emitter and insulator assembly which allows for the thermal expansion differences between the emitter and the collector The collector temperature is measured by two chromel-alumel thermocouples on each end, inserted in the heavy-walled collector and extension

The emitter and collector leads are a composite of one mil molybdenum foils assembled to be flexible in order to permit independent movement of individual diodes sharing a common electrical lead in a hexagonal-shaped cluster of diodes in parallel The cesium reservoir extends from one collector flange and is concentric to the collector and confined within the 1 300 inch outer fuel containment diameter The cesium reservoir is attached to an appropriate heat sink, which, along with the heater, is brazed to the reservoir body and is used to control the reservoir temperature The cesium reservoir temperature is monitored by two chromel-alumel thermocouples imbedded in the reservoir body, these thermocouples were also used for controlling the power input to the heaters

Both the emitter and the collector have an active electrode surface consisting of a thin layer of sublimed material,[1,2] tungsten on the emitter and molybdenum on the collector The expected design point performance at the diode terminal is 6 5 watts/cm^2 at 7 2 amps/cm^2 and at an emitter temperature of 2000°K, with an efficiency of 13% This performance is based on the experimental results from five heat pipe diodes[2] and one planar diode,[1] along with the assumption that the radiation losses from the fuel enclosure are limited to end losses (the case for all but 14% of the diodes in a full-scale reactor)

Figure 4 is a plot of output power density, emitter heat flux, and diode terminal efficiency versus emitter current density, at a constant emitter temperature of 2000°K From this figure it can be seen that the diode terminal efficiency is maximum at a current density of 8 amps/cm^2 The emitter heat flux at 8 amps/cm^2 is about 52 5 watts/cm^2, which is slightly higher than the desired emitter heat flux of 50 watts/cm^2 This heat flux was set as an upper limit based on the thermally induced stresses within the emitter

At an emitter heat flux of 50 watts/cm^2, the terminal diode efficiency is 13 2%, which produces an output power density of 6 5 watts/cm^2 at 7 2 amps/cm^2 Taking this as the design point, the expected diode output power density and terminal efficiency plus emitter temperature for a constant emitter heat flux of 50 watts/cm^2 was calculated, it is shown in Figure 5

The diode performance shown in Figures 4 and 5 was based on uniform current generation along the length of the emitter, rather than on a weighted current generation A sample calculation of the expected diode performance at the design point is found in Appendix A

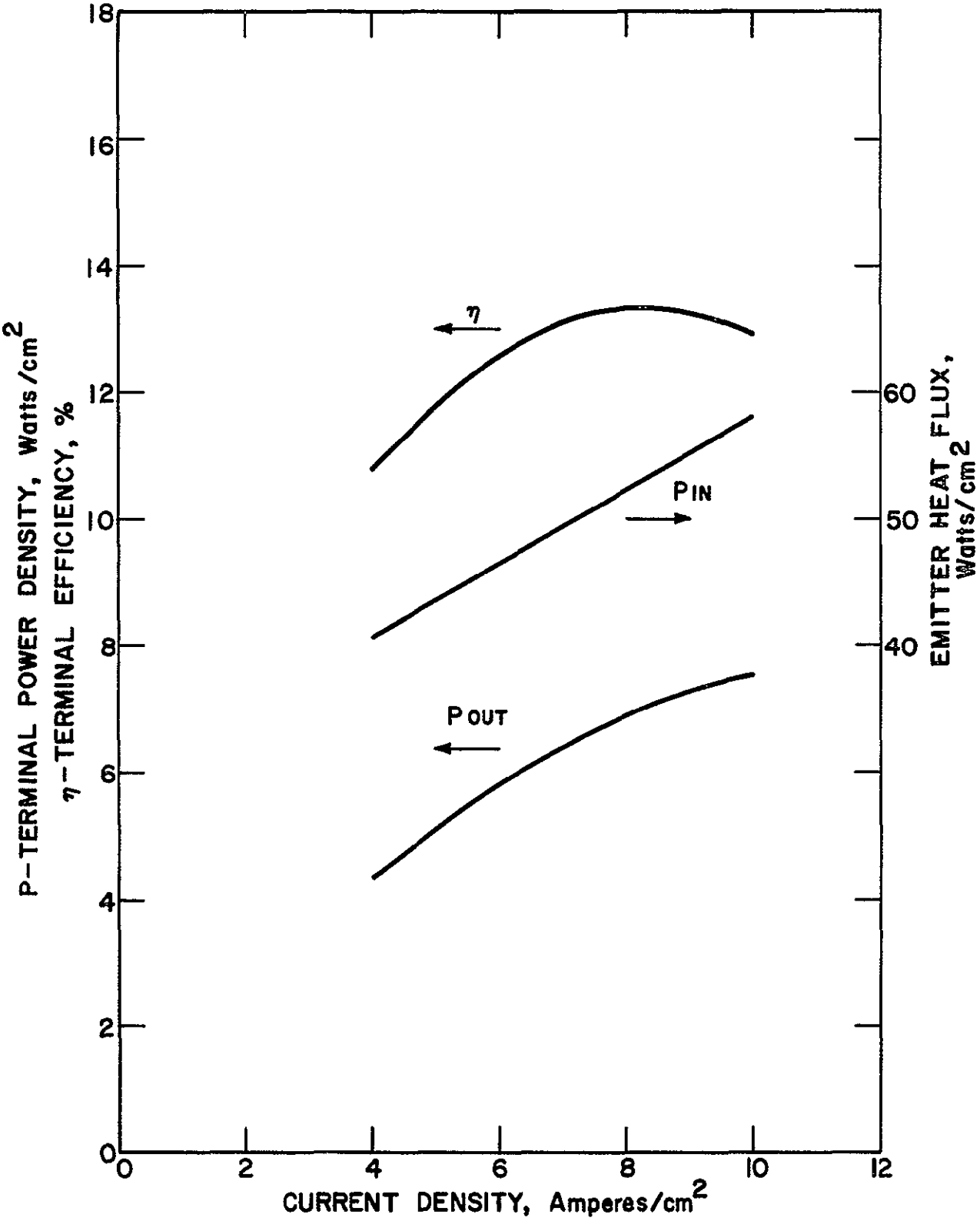

Figure 4 Diode Performance at 2000°K

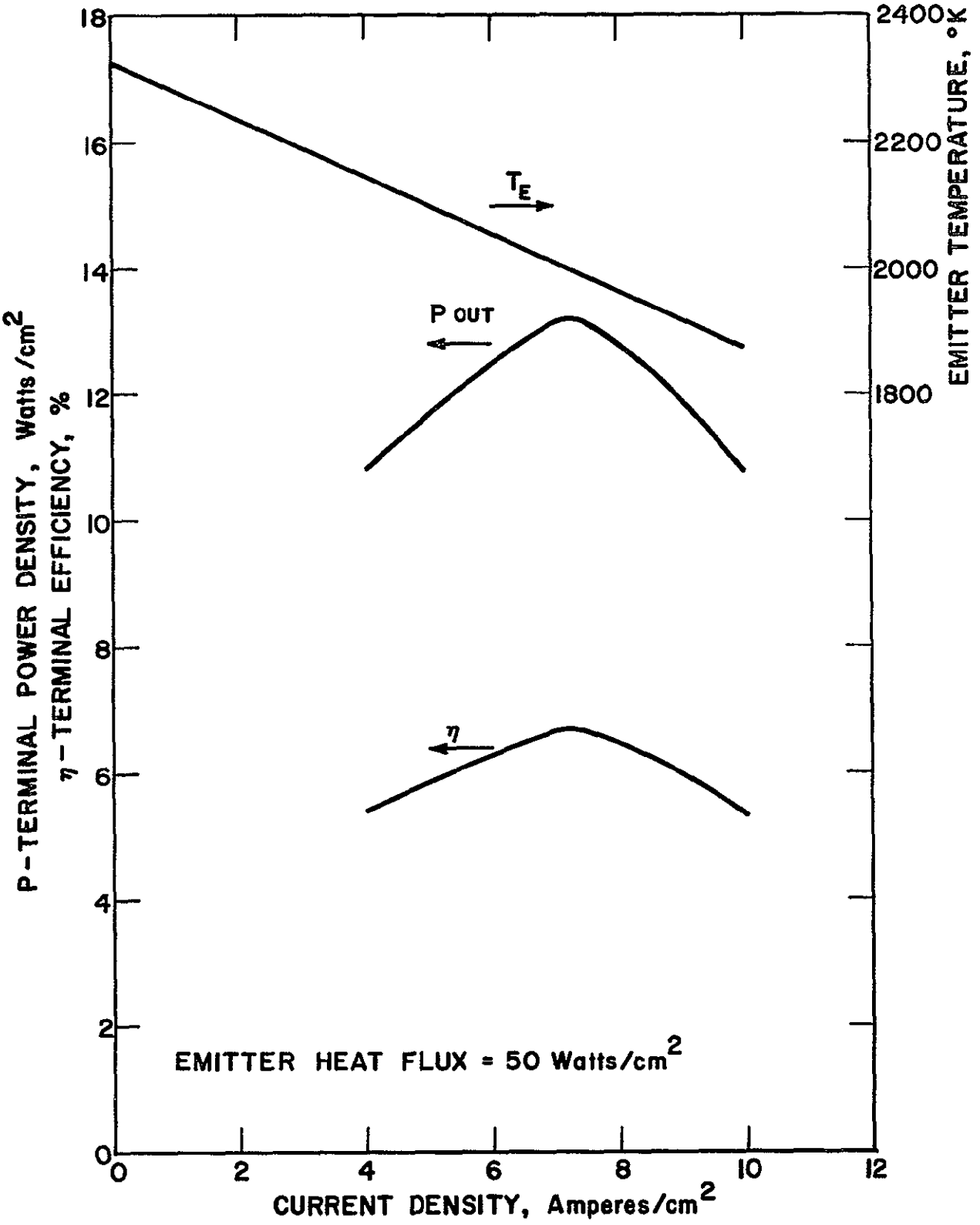

Figure 5 Diode Performance at Design Point

The overall temperature profile for the fueled emitter is seen in Figure 6 These temperatures are for an emitter heat flux of 50 watts/cm^2 and a 0 5 watt/gram gamma heating rate of the fuel enclosure, with the diode operating at the design point of 7 2 amps/cm^2 Increasing the gamma heating rate to 2 5 watts/gram,keeping the other parameters constant, raises the maximum fuel enclosure temperature from 2138°K to 2175°K

B. CAPSULE CONFIGURATION

The capsule configuration is seen in Figure 7 with the full length diode in place The actual diode has not been changed, however, certain additions and modifications were required under the constraints of the in-pile test These include method of cooling the diode, additional instrumentation, and complete double containment of the diode and fission gas container

The method of cooling the cqllector has been changed from a pumped NaK loop to a variable conductance helium gap-to-water system This system requires trim heaters to maintain the necessary heat loss down the collector lead, preventing the collector temperature from being reduced to a value below the cesium reservoir temperature

The net heat loss from the fuel in the radial direction will be reduced by the insertion of 25 one-mil tungsten foils separated by zirconium oxide between the primary and secondary fuel enclosures

The fission gas will be vented from the fuel cavity through the niobium secondary fuel enclosure to a volume of 67 cc at 400°K or less, which will keep the pressure built up at 10, 000 hours to a value less than 100 torr The fission gas pressure will be monitored by a suitable pressure transducer

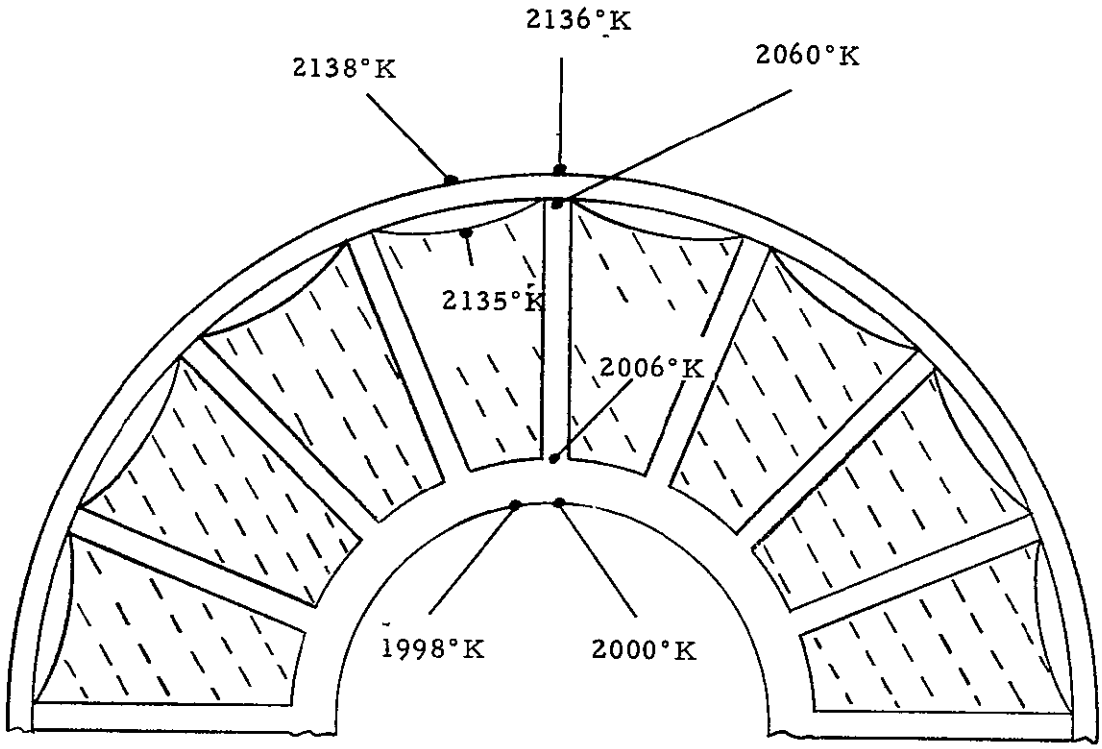

Figure 6 Fueled Emitter Temperature Profile

The entire fuel cavity and fission gas pressure systems will be doubly contained to assure the safety of the experiment The secondary containment will also contain a pressure transducer, which will provide a means of determining if the primary containment develops a gas leak other than into the interelectrode space of the thermionic diode If fission gas enters the cesium envelope of the diode, its presence will be determined by the lowering of the diode's performance

The secondary containment will be made of niobium throughout Specifically, the fuel secondary containment will be a 0 025 inch thick niobium cylinder, with an outer diameter of 1 5 inches, joined to the niobium portion of the emitter sleeve extension through a 0 010 inch thick disked niobium plate The combination of thin cylinder and disk will be flexible enough to compensate for the difference in thermal expansion of the materials The diode will have additional instrumentation, including three rhenium sheathed W-Re 5%/W-Re 26% thermocouples inserted in bosses which are welded directly to the outside of the primary fuel containment. These will penetrate the secondary fuel enclosure and will spiral down the primary fuel enclosure to three different axial locations. The spiraling will provide for the thermal expansion differences of the materials Chromel-alumel thermocouples will be placed within the bosses in the niobium extension of the emitter sleeves and three chromel-alumel thermocouples will be placed on the niobium secondary fuel container

The electrical output will be removed from the diode by water-cooled copper buses Each end of the diode will be independent of the other Thus, there will be two emitter leads and two collector leads The voltage will be determined at the terminals of the diode on each end by emitter and collector voltage taps

All instrumentation and power leads will penetrate the capsule through a seal flange, and will be insulated from the capsule and each other In order to insulate the emitter from the capsule, the primary support of the diode, through the niobium secondary fuel enclosure, will be joined to the niobium secondary fuel enclosure by utilizing a 30% niobium-alumina cermet

The cesium reservoir will be cooled through a thermal impedance path to one of the collector lead cooling buses

The capsule will have an outer diameter of 2 75 inches, allowing assembly clearance within the 3-inch square core matrix The entire capsule will be dynamically pumped with an ion pump The in-pile vacuum system is seen schematically in Figure 8

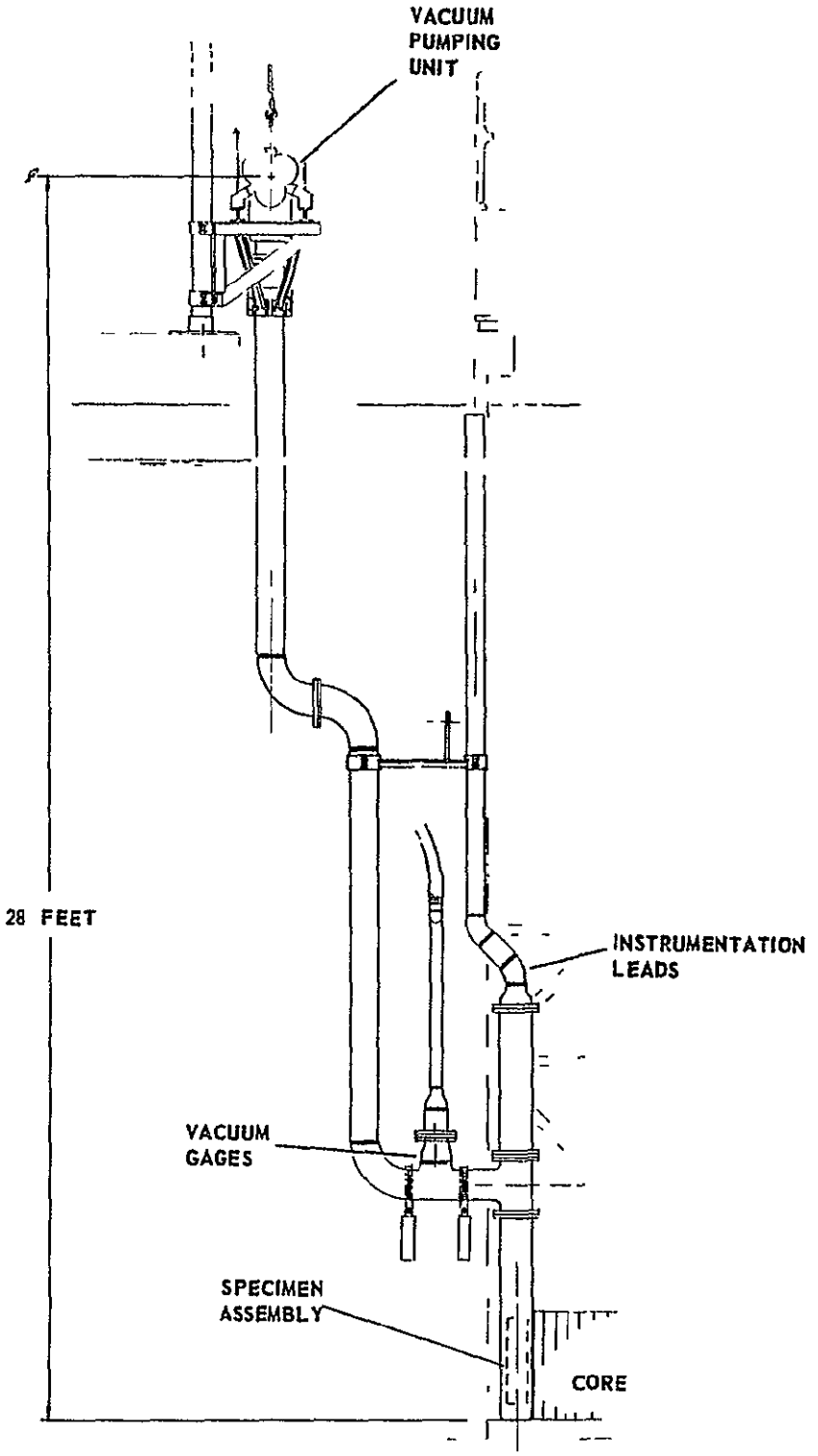

Figure 8 In-Pile Vacuum System

IV FUELED DIODE DESIGN CRITERIA

The overall design of a high fuel volume fraction-external fuel thermionic diode depends strongly on the configuration of the fuel-emitter structure In turn, the fuel-emitter structure design is dictated by the specific choice of fuel material, structural materials, and in part by the absolute dimensions It is the intent of this section to lay the basis for understanding the choice of the unbonded fuel-emitter structure as the primary design, with the bonded fuel-emitter structure as the secondary design

A FUEL CONSIDERATIONS

Ideally, a fuel with high thermal and electrical conductivity such as uranium nitride (UN) or uranium carbide (UC) could be employed With these fuels, the need for additional radial conductivity provided by tungsten webs is no longer present If bonding of the fuel to the emitter is not achieved, then any additional electrical conductivity which is required for the emitter can be added directly to the bulk emitter If UO_2 is desired as the nuclear fuel, then the use of a tungsten or molybdenum cermet would provide the additional radial thermal conductivity, again, the bulk emitter could be increased in diameter to provide the required electrical conductivity

These ideal fuels are just that, and to date each has one or more shortcomings UC's reactivity with air and moisture requires special fabrication, handling and loading procedures in order to assure the purity of the fuel UN is an untried fuel at thermionic temperatures, the possibility of a cover gas of nitrogen introduces an additional design problem The failure of cermets to achieve their potential has been

the unrestricted swelling of the fuels under irradiation Thus, UO_2, with its poor thermal conductivity, must be considered as the most likely fuel to be used Therefore, the design of the fueled diode reflects the use of UO_2 by the inclusion of the tungsten webs attached to the emitter

B EMITTER-FUEL STRUCTURE CONCEPTS

Two basic emitter-fuel concepts were considered in this study The first consists of an all-bonded structure of two concentric cylinders with interconnecting axial webs, with no compensation for differences in thermal expansion of components other than elastic deformation or yielding of structural members The second, also of finned construction, utilizes a floating outer fuel container with flexible end closures to allow for the differences in the thermal expansion of the components

To further explore these two concepts, the following ground rules were established from system constraints

1 The terminal power density should be equal to or greater than 6 watts/cm^2 for a minimum of 100 cm^2 per diode
2 A core (fuel-emitter) length of 10 inches
3 A high fuel fraction, approaching 57 5%, within the smallest volume
4 A maximum fuel temperature of 2150°K

In order to achieve the emitter surface area, an emitter diameter of 0 55 inch was chosen, even though an 0 50 inch diameter would have sufficed The additional 0. 050 inch in diameter was utilized on the collector to reduce ohmic losses, while allowing for

sufficient internal collector coolant passage The collector has an inner diameter of 0 300 inch and an outer diameter of 0 530 inch The thickness of the emitter was chosen to be 0 060 inch for structural reasons At this point the design of the emitter-fuel structure becomes relevant A parametric analysis was done for the two design concepts The fuel fraction, the ohmic losses within the emitter-fuel structure, the thermal gradient through the emitter webs, and the maximum fuel temperature were looked at with respect to the number and thickness of the emitter webs, along with small variations in the outer fuel enclosure diameter and thickness For the analysis, the emitter temperature was set at 2000°K with an emitter heat flux of 50 watts/cm^2 Figures 9 and 10 show the results of the analysis for the two outer fuel enclosure diameters and thicknesses which were ultimately chosen for the two designs, one of each concept, to be evaluated further

From Figures 9 and 10 it can be seen that a bonded design of eight interconnecting tungsten webs is about equivalent to an unbonded design of 16 tungsten webs, and that both of these are the minimum number of webs possible for the particular concept because of the fuel temperature limitations The one distinct difference between the two design concepts at the minimum number of webs is the temperature through the tungsten webs

Both bonded and unbonded designs are dimensionalized in Figure 11 and Table I Also tabulated are the resistive losses in the emitter at 7 2 amps/cm^2, the maximum available fuel fraction, the temperature gradient through the webs, the maximum fuel enclosure temperature, and the maximum fuel temperature For the sake of

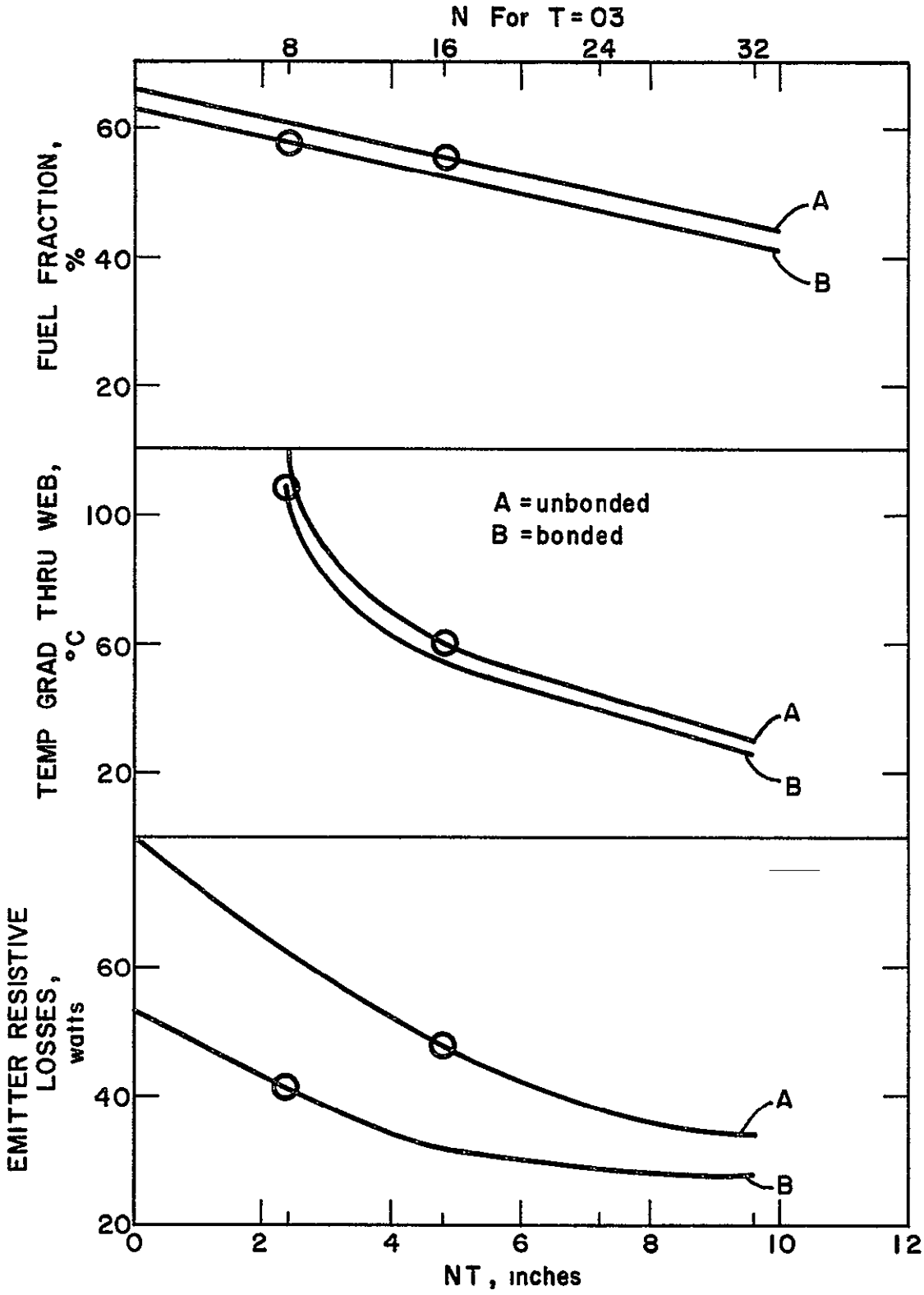

Figure 9 Fuel Fraction, Temperature Gradient, and Ohmic Losses at Maximum Fuel Temperature versus the Number and Thickness of the Webs

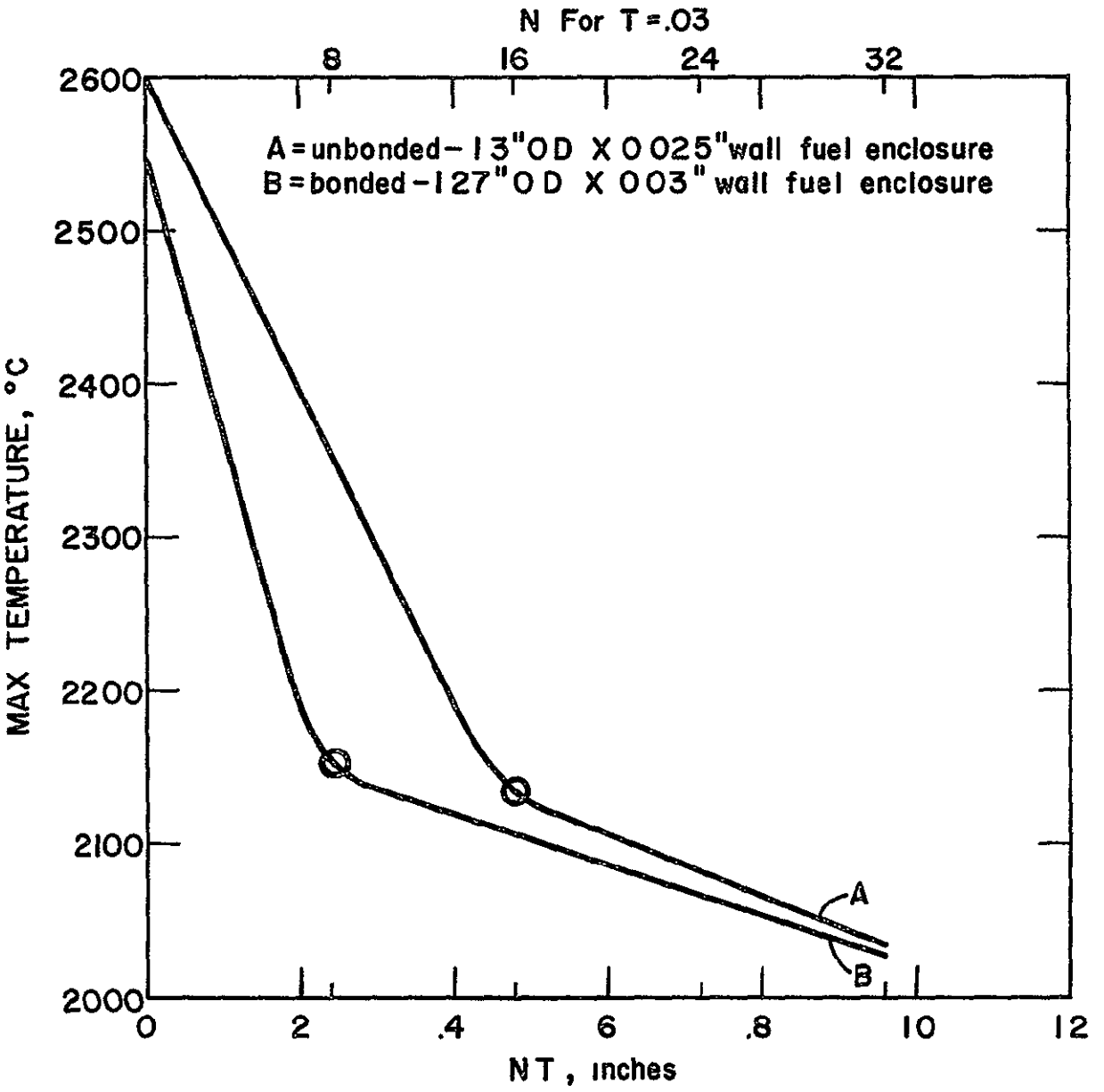

Figure 10 Fuel Fraction, Temperature Gradient, Ohmic Losses and Maximum Fuel Temperature versus the Number and Thickness of the Webs

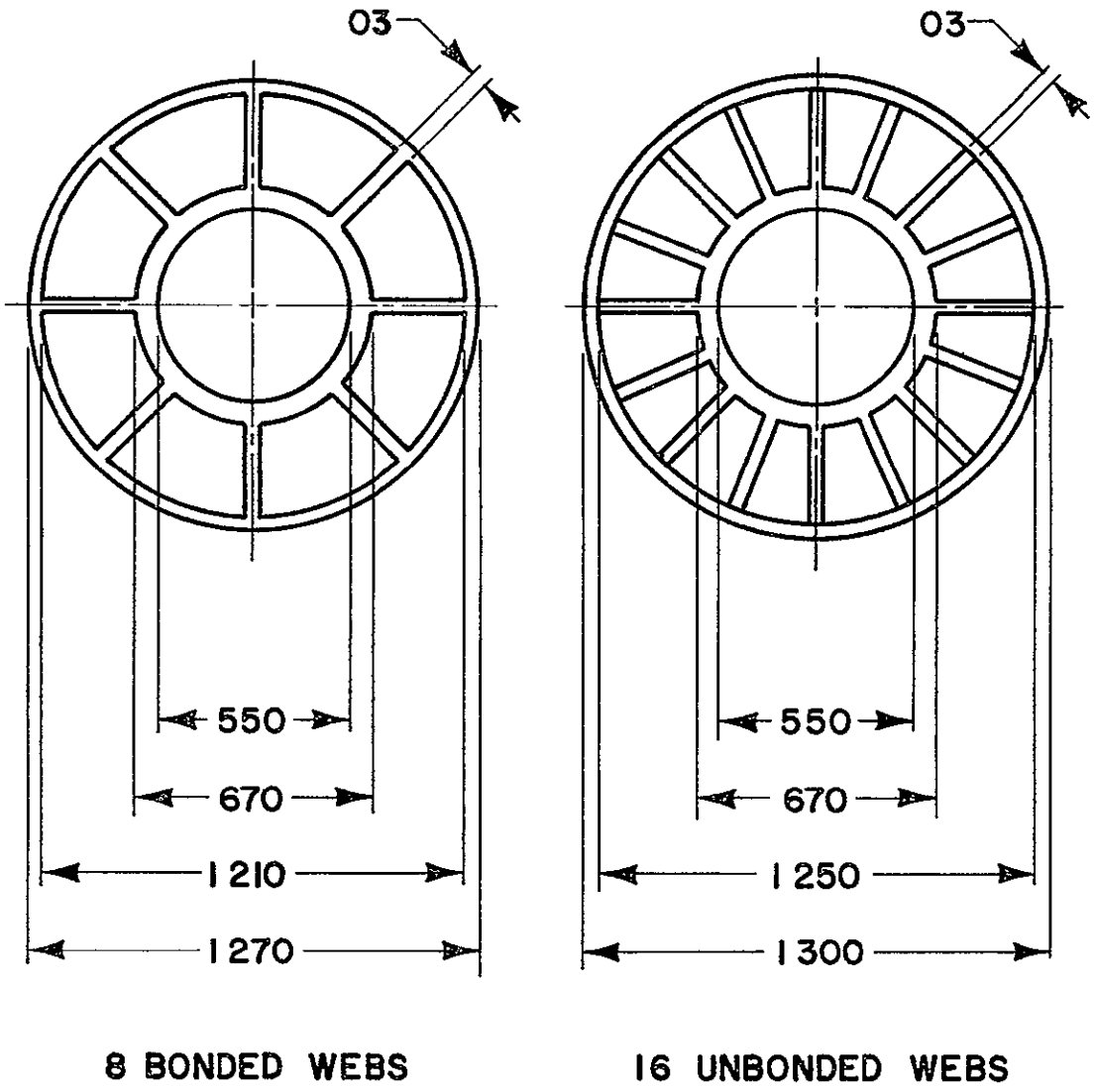

Figure 11 Emitter Design Dimensions

TABLE I

EMITTER-FUEL STRUCTURE COMPARISON

	Component Description - 2000°K Emitter Temperature - 50 w/cm^2 Emitter Heat Flux	Emitter-Fuel Configuration		
		Revolver	Bonded	Unbonded
1	Outer fuel container diameter - inches	1 5	1 27	1 30
2	Number of radial webs	6	8	16
3	Thickness of radial webs-inches	0 I35	0 030	0 030
4	Outer fuel container thickness - inches	0 040	0 030	0 025
5	Emitter thickness - inches	0 060	0 060	0 060
6	Emitter diameter - inches	0 500	0 550	0 550
7	Maximum available fuel fraction, %	44	57 5	55 7
8	Emitter surface area - cm^2	101	111	111
9	Resistive losses in emitter at 7 2 amps/cm - watts	10	42	46
10	Temperature gradient through web at 50 watts/cm^2-°C	30	109	59
11	Maximum fuel enclosure temperature, °K	2090	2135	2138*
12	Maximum fuel temperature, °K	2140	2149	2135

*This includes dissipation of 0 5 watt/gram gamma heating of the floating fuel enclosure

further comparison, some of the pertinent design criteria of the lower fuel fraction revolver diode are also included in Table I

Each of the two designs has certain advantages and disadvantages, some of which are seen in Table I and Figures 9 and 10 The all-bonded structure must be fueled prior to diode construction and, therefore, is electrically tested with the fuel in place During electrical testing, however, the allowable heat flux through the emitter may be limited, since the thermal gradient and the resultant thermal stress through the fuel and webs are greater for external heat generation (electrical) than for internal heat generation (nuclear) While the all-bonded design is more difficult to fabricate and is subjected to higher stresses, it exhibits lower electrical losses and would probably result in an overall simpler fueled diode design.

The unbonded design can be fueled after the diode has been fully assembled and electrically tested to the required heat fluxes If testing of the diode with fuel in place is desired, it can be retested at a lower heat flux to demonstrate that fueling has not damaged the diode The electrical resistance of the unbonded design is slightly higher than that of the bonded design, however, the stress within the webs is considerably reduced, the end closures are designed to be flexible members, and the maximum fuel and fuel enclosure temperatures are similar to the bonded design

It is obvious from Table I that the major distinction between the two designs is the temperature gradient through the tungsten webs This was the deciding factor in picking the unbonded design as the primary design The temperature gradient through the restrained

webs in the bonded design results in stresses within the entire structure which exceed the yield strength of the materials The reduction in this gradient through the unrestrained web in the unbonded design, combined with the flexibility of the end closures, reduces the stresses throughout the structure to an acceptable level

A detailed discussion of the stress analysis of the two designs is found in Section V

V EMITTER FUEL STRUCTURE STRESS ANALYSIS

The two designs evaluated were the all-bonded structure with eight interconnecting webs, and the unbonded design with 16 webs The unbonded design has two distinct advantages over the bonded design a lower temperature gradient through the tungsten webs, and flexible end enclosures Both of these could be included in the bonded design by increasing the number of webs to 16 and by adding the flexible end members However, the fact that the tungsten webs are not attached to the outer fuel enclosure in the unbonded design has yet another advantage, that of substantially reducing the stresses within the structure It is this factor that truly differentiates between the two designs

It is the intent of this section to present a stress analysis for the bonded design The analysis, although complicated by mathematics, will be presented without the actual computations All necessary formulas and material constants will be presented, along with a discussion of the results

A SUMMARY

The all-bonded emitter fuel structure, after numerous thermal cycles from room temperature to operating temperature and back again, was stressed when at room temperature up to a level of 31, 000 psi in the outer fuel enclosure, with permanent deformation of the outer fuel enclosure of up to 4×10^{-4} inches on a radius This deformation may take place as an inward movement of the outer fuel enclosure at the point of contact of the webs, or as some outward movement of the outer fuel enclosure at the midpoints between the

webs The possibility of joint fracture depends upon the strength of the bond between the webs and the outer fuel enclosure

B BONDED STRUCTURE

The dimensions for the bonded structure are shown in Figure 11 The heat generated within the fuel is equivalent to 50 watts/cm^2 at the emitter surface, which generates the temperature profile seen in Figure 12 The calculation of the stress level and the amount of elastic and plastic deformation is carried out for various cases In all cases, the temperature gradient through the web is assumed to be linear with the outer fuel enclosure temperature, i e ,

$$\Delta T_{web} = \frac{109}{1869} T_{can} = 0\ 0584\ T_{can}$$

The outer fuel enclosure temperature is always at the higher temperature Also, it is assumed that there is no longitudinal temperature gradient in the fuel-emitter structures

There are many stresses developed throughout the emitter-fuel structure The two which differentiate between the bonded and the unbonded design are

a The resultant stress caused by the temperature gradient through the webs and the fact that the webs are bonded to the outer fuel can

b The massive end closures sealing off the fuel cavity

The remaining stresses, which are similar for the two designs, are

c The circumferential and longitudinal stresses due to the temperature gradient through the emitter wall thickness

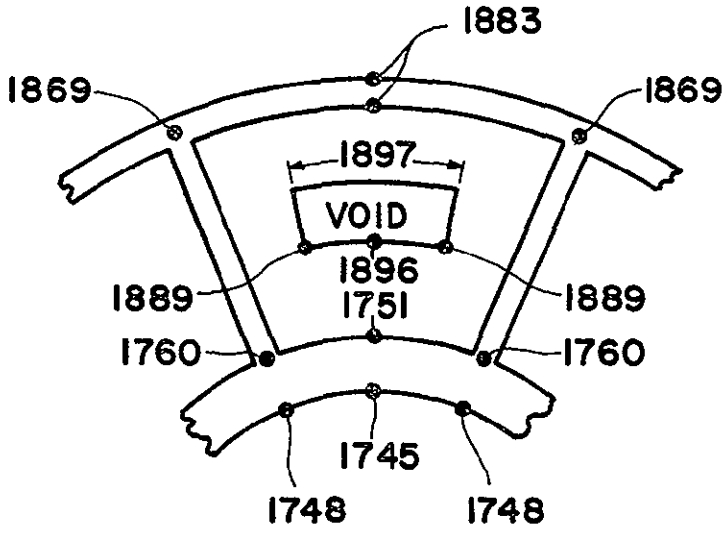

TEMPERATURE, °C
AVERAGE EMITTER HEAT FLUX, 50 Watts/cm^2
VOID, 15 %

Figure 12 Bonded Emitter Temperature Profile

d The temperature gradient through the webs, which gives rise to a bonding stress along the length of the webs

1 Web Gradient

Case 1 Room Temperature-to-Operating Temperature

Under an increasing temperature gradient through the webs, the following condition exists The outer fuel enclosure wants to expand at a faster rate than the webs and emitter will allow it, thus, the emitter and webs are put in tension and the outer fuel enclosure is put in compression

The radial displacement of a cylinder under any number of equally spaced radial forces, either compression or tension, is given by Roark [3]

$$dR = \frac{WR^3}{2EI}\left[\frac{1}{\sin^2\theta}\left(\frac{1}{2}\theta + \frac{1}{2}\sin\theta\cos\theta\right) - \frac{1}{\theta}\right] \qquad (1)$$

The radial displacement for the cylinder at the midpoint between the loads is

$$dR = \frac{WR^3}{4EI}\left[\frac{2}{\theta} - \frac{1}{\sin\theta} - \frac{\theta\cos\theta}{\sin^2\theta}\right] \qquad (2)$$

Also, a bending moment exists in the cylinder The positive moment is maximum at the midpoints between the loads and is equal to

$$M = \frac{1}{2}WR\left(\frac{1}{\sin\theta} - \frac{1}{\theta}\right) \qquad (3)$$

The negative moment is maximum at the level points and is equal to

$$M = -\frac{1}{2} WR \left(\frac{1}{\theta} - \cot \theta\right), \tag{4}$$

$$\sigma = \frac{MC}{I} = \epsilon E = \frac{dR}{R} E \tag{5}$$

Thus, the radial deflection caused by a moment is

$$dR = \frac{RMC}{IE} \tag{6}$$

Calculations of these moments for the emitter and the fuel can show that the maximum moment, either positive or negative, occurs at each load point and the resultant induced stress and radial displacement is 2000 times greater than that computed using formula (1)

The stress in a single web is

$$\sigma_w = \epsilon E = \frac{W}{LI} \tag{7}$$

The width of the webs at any temperature is

$$\ell_w = (R_2 - R_1)(1 + \alpha_{12} \Delta T_{12}) \tag{8}$$

Thus, since $\epsilon = \frac{\Delta \ell}{\ell}$, the amount of deflection in a web for a given load is

$$\Delta \ell_w = \frac{W \ell}{LIE} = \frac{W(R_2 - R_1)(1 + \alpha_{12} \Delta T_{12})}{ELI} \tag{9}$$

The total amount of deflection which would be necessary if the web was not connected to the outer fuel enclosure is

$$\Delta \ell_t = R_2(1 + \alpha_2 \Delta T_2) - R_1(1 + \alpha_1 \Delta T_1) + (R_2 - R_1)\ (1 + \alpha_{12} \Delta T_{12}), \qquad (10)$$

which can be shown to be

$$\Delta \ell_t = \frac{R_2 + R_1}{2} (\alpha_2 \Delta T_2 - \alpha_1 \Delta T_1) \qquad (11)$$

At any given temperature, the total amount of deflection must be the sum of the three individual components Thus,

$$\Delta \ell_t = dR_e + d\ell_w + dR_c \qquad (12)$$

Using equation 12 and substitution equations 9 and 6, along with the fact that the loading W must be equal throughout the system, provides a solution for W, the load at any given temperature From the value of W, the amount of deflection in each component can be found, as well as the stress level

Figure 13 shows the thermal expansion of tungsten versus temperature, along with a plot of equation 11, the total required deflection versus temperature, and a plot of the temperature gradient through the webs versus temperature From the resulting equations, calculations were made at various temperatures

The elastic deformation of the three components is as follows The emitter and webs of each deform 5 percent of the total, while the outer fuel can deforms the remaining 90 percent Figure 14 shows a plot of the maximum stress in the outer fuel can versus temperature, along with the 0 02 percent offset yield strength for wrought tungsten As can be seen, at a temperature near 1500°C the maximum stress in the can exceeds the yield strength, thus, the can begins to yield

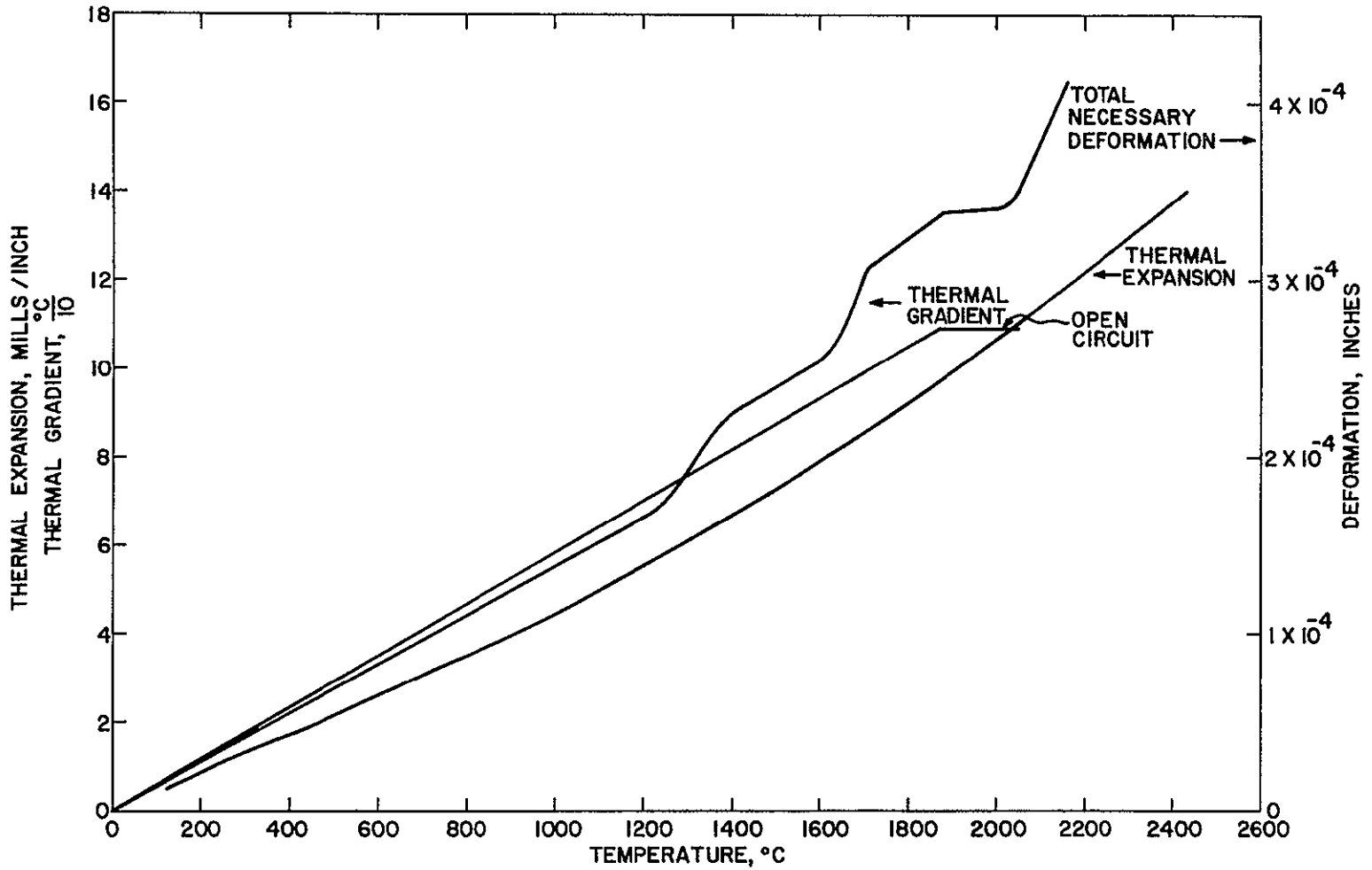

Figure 13 Thermal Characteristics of Tungsten and Tungsten Emitters

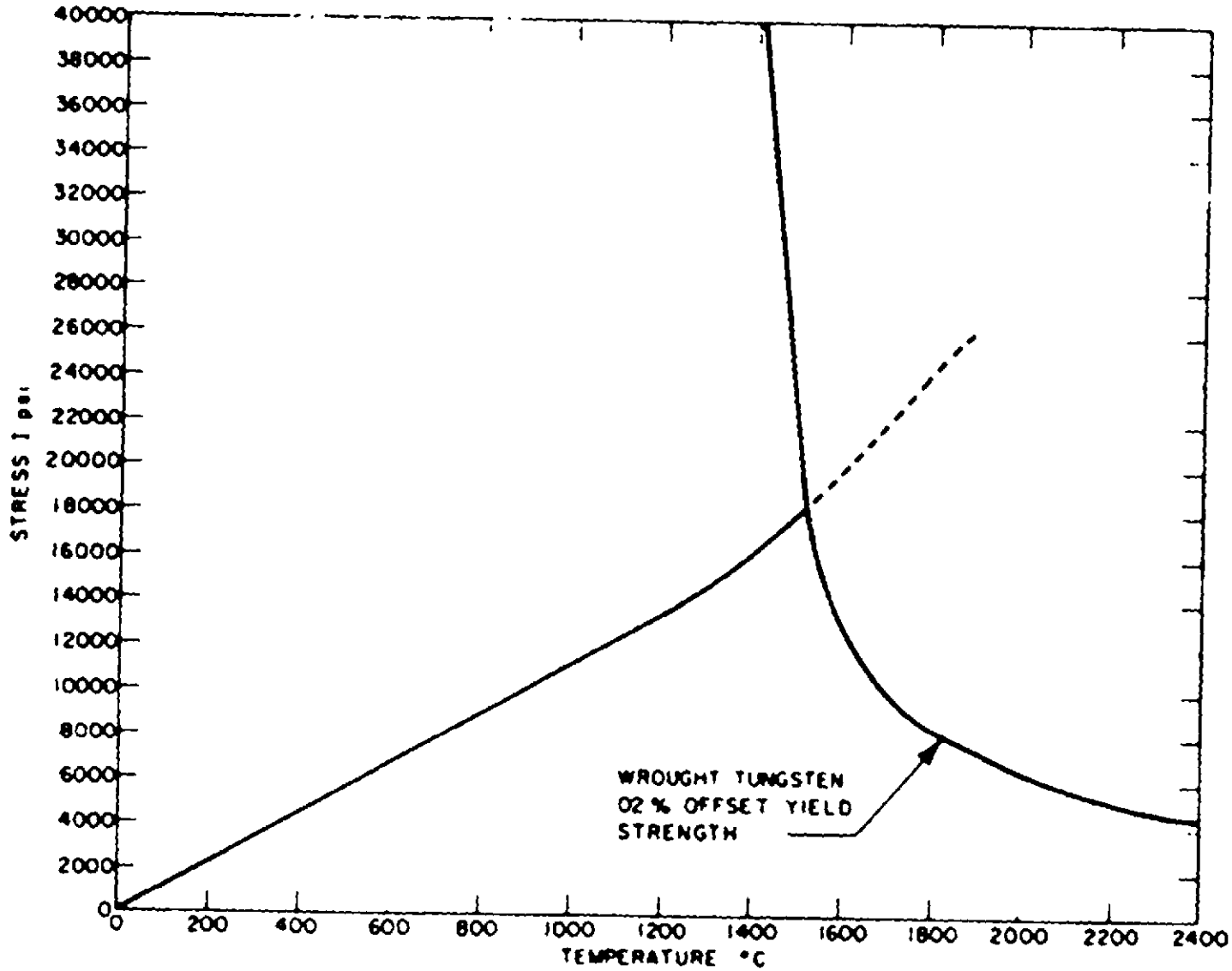

Figure 14 Stress versus temperature

The temperature at which complete yielding occurs was determined as follows The maximum allowable bending moment at any temperature and the actual bending moment within the can for the same temperatures were ascertained These were then plotted versus temperature (shown in Figure 15), and were found to intersect near 1600°C, where complete yielding will occur in the outer fuel can

The maximum bending moment for the can is

$$M_m = \frac{Lt^3}{4} \sigma_{y\ s.}, \qquad (13)$$

which is shown along with equation 4 in Figure 15

Thus, as the temperature increases from 1500 to 1600°C, the outer fuel can continues to yield until complete yielding occurs At this point, as the temperature increases, the amount of stress which can be accommodated is the yield strength The outer can continues to yield to a stress level of 7500 psi at 1869°C, where the amount of elastic deformation is small (equivalent to a loading which gives rise to a 7500 psi stress level) and the rest of the deformation is inelastic or permanent

If this temperature is maintained for any length of time, the outer fuel can will creep until the stress level in the can approaches zero at an infinite time From the known creep rate of tungsten at these temperatures, the stress level should be essentially zero (less than 500 psi) after a few hours Thus, the total deflection of 3.4×10^{-4} inches on a radius is permanent deformation of the outer fuel can in the inward direction

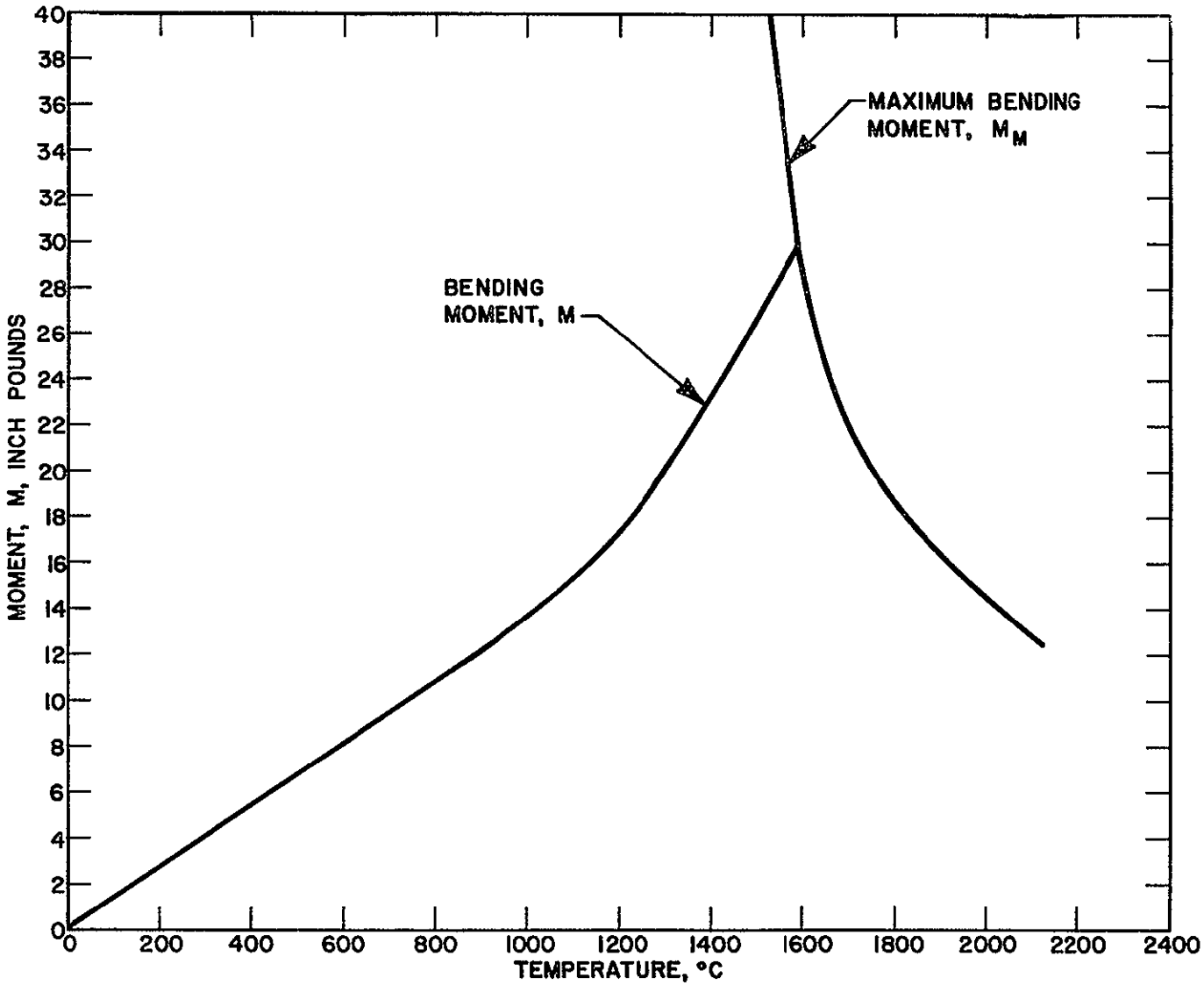

Figure 15 Bending Moment versus Temperature

The same reasoning applies if the outer fuel can goes to 2159°C, the open circuit condition, except the total deflection is now 4 1 x 10^{-4} inches/radius

Even though the stress analysis shows that the outer fuel enclosure will yield at the load points, the fact that the outer fuel enclosure is attached to the webs will probably enhance the strength at the load points Thus, there is the possibility that part or all of the deformation of the outer fuel enclosure will come at the midpoint between the loads

If the outer fuel enclosure yields outward at the midpoints between the webs, rather than inward at the webs, the total amount of deformation of the midpoint plus any deformation at the webs will still be equal to 3 4 or 4 1 x 10^{-4} inches, which is the maximum required amount for normal operating or open circuit conditions

The outward deformation of the outer fuel container at the midpoint between the webs is enhanced by the fact that the midpoint operates 13°C higher than at the webs This temperature gradient in the outer fuel container gives rise to a circumferential tensile stress in the outer fuel container and is equal to

$$\sigma = E\alpha\Delta T,$$

which amounts to 3000 psi for normal operating conditions This 3000 psi stress will be relieved by creep as time passes, since there is a normal tendency for the outer fuel can to move outward at the midpoint, the creep will also be outward The amount of deformation associated with the creep will be small (2 x 10^{-5} inches), which is about 20% more

than the permanent deformation due to the temperature gradient through the webs

Case II Cooldown from 1869°C to Room Temperature

Upon cooling, the reverse situation occurs The outer fuel can, which has been deformed, wants to move inward further than the emitter and webs will allow it, thus, the emitter and webs go into compression and the outer fuel can goes into tension

Now that the tungsten has been fully recrystallized, the 0 02% offset yield strength is much lower, as shown in Figure 16 As the structure cools, the maximum stress in the outer fuel can may build up to a maximum value of 29,000 psi at room temperature, during which time it always remains below the maximum allowable yield strength (as seen in Figure 16) However, in the 1400-1800°C range, the stress levels are high enough that some creep may occur The extent of this creep is quite difficult to predict Thus, the structure will probably be stressed at 29,000 psi when at room temperature

Cooling down to room temperature from open circuit conditions of 2159°C causes a bit more yielding and possibly more creep to occur, as seen in Figure 16 If open circuit conditions are achieved long enough for the stress level to become essentially zero, the room temperature stress is 37,000 psi There is then a range from 1800°C to 800°C where the maximum stress is higher than the yield strength, so some yielding of the can does occur, though it is not complete This partial yielding, along with creep at the higher temperatures, may cause some permanent deformation during the cooling cycle if the cooling time is long However, this is very difficult to predict and will probably not be much more than 10% of the total deflection

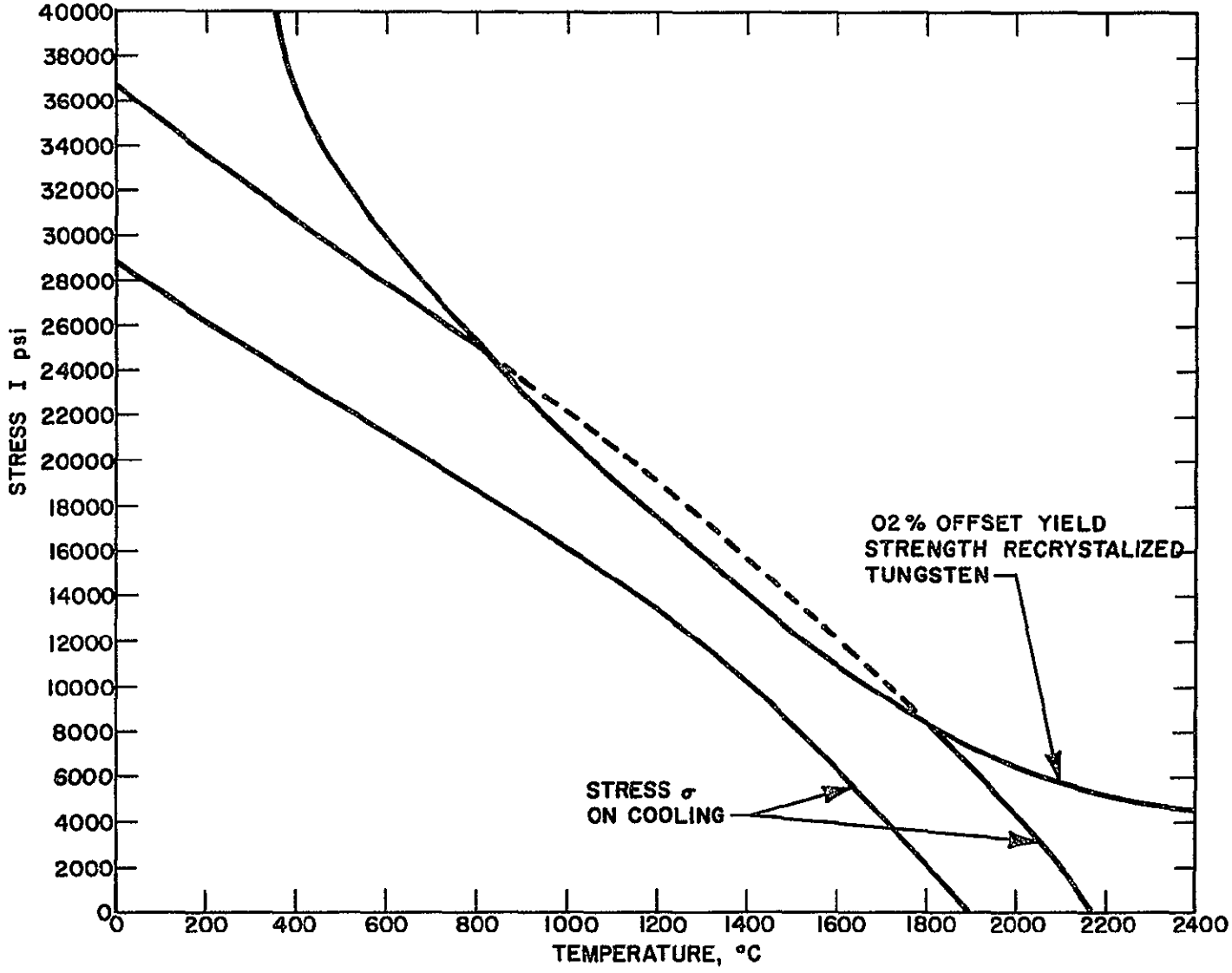

Figure 16 Stress versus Temperature

Case III Second and Succeeding Cycles to 1869 or 2159°C

If there is no yielding or creep of the outer fuel can during the cooling cycle, then, as the structure is reheated, the stress levels reduce themselves as the temperature is increased and become zero at operating temperature If, however, there was a small amount of yielding and creeping on the cooldown cycle, then the stress level goes through zero and builds up in the outer fuel can at operating temperature This stress can then be reduced to zero by creep, as in Case I.

Case IV Second and Succeeding Cooldown Cycles from 1869 or 2159°C

During these cooldowns, the stress levels will build up as for Case II Possibly there will be some small amount of yielding and creep as the temperature reaches the 1400 - 1800°C range

The net result of numerous thermal cycles will be as follows

a On the first cycle from room temperature to the operating temperature of 1869°C, the outer fuel can will permanently deform the total required deflection of 3 4 x 10^{-4} inches or a radius in the inward direction at the load point (webs) or outward at the midpoints between the webs If the structure goes to open circuit conditions of 2159°C on the outer fuel can and the total deflection is 4 1 x 10^{-4} inches per radius, the additional 0 7 x 10^{-4} inch becomes permanent if the temperature is maintained long enough for creep to occur

b On the first and any succeeding cooldown cycles, there is a possibility of some permanent deformation of the outer fuel can in the outward direction at the webs, or in the

inward direction of the midpoint between the webs The amount of permanent deflection will probably be no more than 0 3 to 0 4 x 10^{-4} inch As the structure cools to room temperature, the stress level will build up in the outer fuel can to a maximum value of 39, 000 psi, which is the case for cooldown from 2159°C without any permanent deformation on the cooling cycle

c On any succeeding heating cycle, the stress level reduces itself to zero at operating temperature, unless there is some permanent deflection on the last cooling cycle The amount of deformation which takes place during the cooling cycle will be reversed and the outer fuel can will again deform by the same amount as in Case I, until the stress level goes to zero

d There is one more possibility On the first thermal cycle, the stress level at the joint between the outer fuel enclosure and the webs may be stressed to failure before the outer fuel enclosure can yield

C END CLOSURES

The end closures over the fuel cavity have the same temperature gradient that the webs have This gradient produces radial as well as tangential stresses The gradient also deflects the end closures, since the outer fuel container expands more than the emitter

The radial stress is zero at both the inner diameter, the outer diameter, and at points between, it is shown by [4]

$$\sigma_r = \frac{-E\alpha}{r^2} \int_a^r T\, r dr + \frac{E\alpha}{b^2 - a^2} \left(1 - \frac{a^2}{r^2}\right) \int_a^b T\, r dr$$

where

$$T = \frac{T_b - T_a}{b - a} (r - a)$$

The radial stress is a maximum at r = 0 5025, for a = 0 335 and b = 0 605 However, this radial stress is only 90 psi tension

The tangential stress is given by

$$\sigma_\theta = E\alpha \frac{1}{r^2}\left[\int_a^r T\, r dr - T\right] + \frac{E\alpha}{b^2 - a^2} \left(1 + \frac{a^2}{r^2}\right) \int_a^b T\, r dr$$

and equals 1080 psi tension at r = a and 612 psi compression at r = b

The radial stress on the end closure at the emitter diameter which results from the difference in the expansion of the emitter and outer fuel can is given by

$$\sigma_r = \frac{3w}{2\pi l^2}\left[\frac{2a^2(m+1)\log\frac{a}{b} + a^2(m-1) - b^2(m-1)}{a^2(m+1) + b^2(m-1)}\right],$$

where W can be found from the maximum deflection at the outer edge

$$Y = \frac{-3w(m^2 - 1)}{4m^2 \pi EI^3} \quad x$$

$$\left(\frac{a^4(3m+1) - b^4(m-1) - 2a^2b^2(m+1) - 8ma^2b^2\log\frac{a}{b} - 4a^2b^2(m+1)(\log\frac{a}{b})}{a^2(m+1) + b^2(m-1)}\right)$$

The maximum longitudinal deflection y is found by the difference in thermal expansion of the emitter and outer fuel can by

$$y = L(\alpha_2 \Delta T_2 - \alpha_1 \Delta T_1)$$

This amounts to 3.5×10^{-3} inches per end when the emitter is at 1760°C and the outer can is at 1869°C

For an end closure 0.03 inch thick, this longitudinal deflection causes a radial tensile stress of 20,000 psi at 1550°C, which is the yield strength at 1550°C For wrought tungsten, therefore, the end closure will yield to a stress level of 9000 psi at 1760°C, which is the yield strength at 1760°C This residual stress will, in the case of the webs and outer fuel container, cause the end closure to creep as the elapsed time period increases The radial elongation of the end closure, which is a combination of yielding and creeping, amounts to 1.2×10^{-4} inches when the stress level has been reduced to zero

If the end closure is thicker than 0.03 inch, then the stress level is higher at a given temperature Accordingly, the end closure yields at a lower temperature However, the end result is complete deformation as time is allowed to increase to infinity The total radial deflection for an end closure 0.05 inch thick is 2×10^{-4} inch In all cases, for virtually any end cap thickness, the end cap will yield since the stress level is in the emitter near the end cap attachment and is approximately 70 percent of the stress level in the end cap However, since the end cap has to be welded to the emitter, there is a distinct possibility that the stress levels will cause the weld to crack rather than causing the end cap to deform

Upon cooling, the reverse situation occurs, and the end cap will be put into a compressive radial stress at the emitter This stress level will be 26, 000 psi for a 0 03 inch thick end cap and would be 43, 000 psi for a 0 05 inch thick end cap However, the higher stress in the 0 05 inch thick end cap will cause yielding to take place at as low a temperature as 800°C, where the recrystallized yield strength is 26, 000 psi However, the amount of yielding will be quite small and the residual stress will still be near 43, 000 psi

D TEMPERATURE GRADIENT AND EMITTER WALL THICKNESS

The temperature gradient through the emitter wall causes a circumferential and longitudinal tensile stress on the emitter surface and a circumferential and longitudinal compressive stress at the fuel surface The stress is

$$T = 1/2\ \Delta T\ \alpha\ E\ (1 - \nu)$$

At 50 watts/cm^2 heat flux, the maximum ΔT is 12°C, and the stress equals 2200 psi This stress level never reaches the yield strength and only creep can take place with time As creep does take place, the emitter surface will have the tendency to increase in diameter and length However, the amount of elongation which may take place is quite small

E TEMPERATURE GRADIENT AND WEBS

The temperature gradient through the webs gives rise to a bending stress along the length of the web This stress is

$$T = 1/2\ \Delta T\ \alpha\ E,$$

compression at the fuel enclosure joint and tension at the emitter joint This 1400 psi stress will be along the interface between the webs and emitter and outer fuel enclosure, and will have the tendency to cause failure of the joints

F UNBONDED STRUCTURE

The stresses in the unbonded structure which are similar to those in the bonded structure are the stress in the emitter due to the temperature gradient and the bending stress in the webs due to the temperature gradient through the web However, since there are 16 webs in the unbonded design, these temperature gradients are approximately half of the gradient in the bonded design Thus, the stress levels are approximately half of those in the bonded design The unbonded structure is never stressed to a level which exceeds the yield strength of tungsten Accordingly, there is no yielding of the structural members other than a small amount of creep which will reduce the low stress levels

VI TEST RESULTS - EMITTER FUEL STRUCTURE

In Section V, the stress analysis showed that the all-bonded design should undergo some permanent deformation when thermally cycled It was also shown that the emitter-fuel structure will normally be highly stressed at room temperature after thermal cycling, and that any unnecessary impulses applied to the system might cause fracturing of the structure Although the all-bonded structure should be deformed and stressed, it inherently provides the simplest overall fueled diode structure Accordingly, it was decided that the all-bonded structure should be investigated to find a means of fabricating and thermal cycling actual components, and to determine the exact extent of the findings of the stress analysis

In order to investigate the all-bonded structure fully, 3 three-inch long (fuel-length) tungsten emitters were fabricated by the following methods

a EDM entirely from an arc-cast tungsten billet

b CVD inside and outside cylinders onto prefabricated tungsten webs made from vacuum arc-cast sheet

c Make the inner cylinder and webs from an arc-cast tungsten billet, CVD the outer cylinder

These three fabrication techniques are shown in engineering drawings in Figures 17, 18 and 19 Figure 20 shows two views of the arc-cast fuel-emitter structure after machining Figure 21 shows two views of the same structure with the niobium end flanges welded in place

FOLDOUT FRAME 1

FOLDOUT FRAME 2

HOLE	DESCRIPTION	DRG	NO OF HOLES

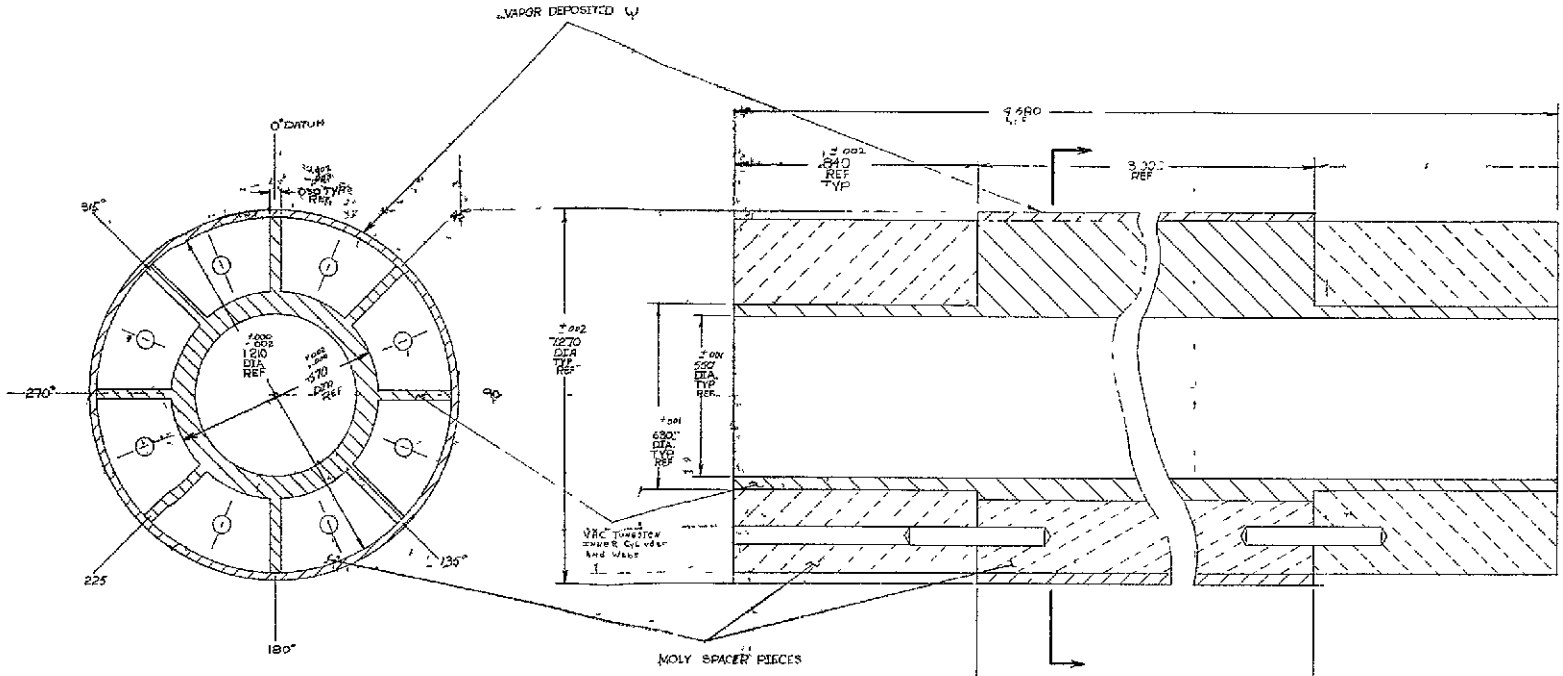

REVISIONS

MATERIAL		THERMO ELECTRON CORPORATION 85 FIRST AVENUE WALTHAM MASSACHUSETTS 02154	
FINISH		UNLESS OTHERWISE SPECIFIED	DRAWN / DATE / CHECKED
NO REQUIRED		FRACTIONAL ± .02 DECIMAL .XX ± .01 .XXX ± .005 FILLET RADIUS .010 MAXIMUM THREADS CLASS 2 ALL DIAMETERS CONCENTRIC WITHIN .005 T I R SURFACES TO BE PERPENDICULAR WITHIN .005 T I R SURFACES TO BE PARALLEL WITHIN .005 T I R HOLE ANGULAR TOLERANCE ± 0°15' ALL OTHER ANGULAR TOLERANCE TO BE ± 0°30' REMOVE ALL BURRS AND EDGES	TITLE FIGURE 19 FABRICATION TECHNIQUES FOR HYBRID TUNGSTEN-FUEL-EMITTER
NEXT ASSEMBLY			SIZE D / DRAWING NUMBER 85-SK2 / SHEET 1 / REV -

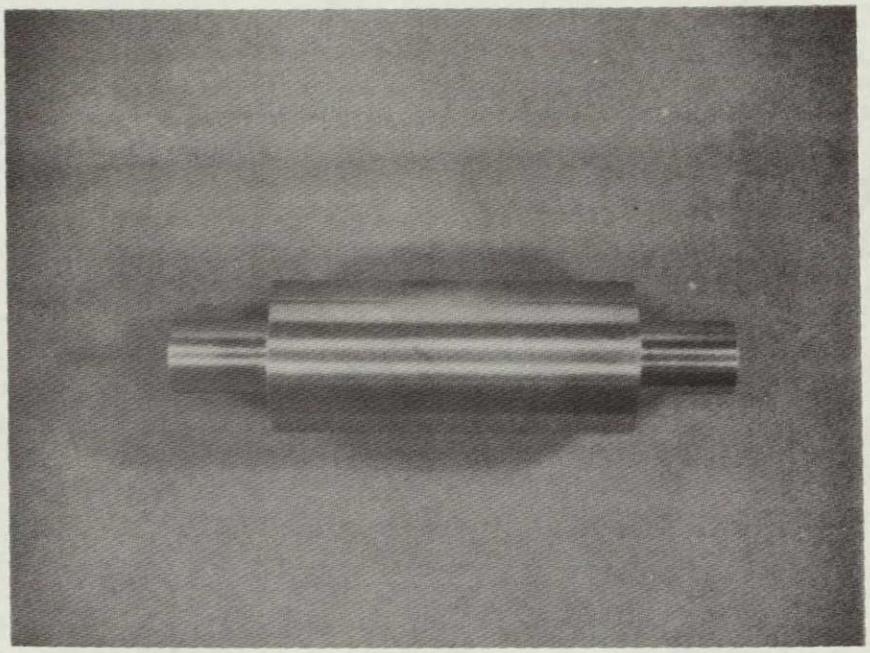

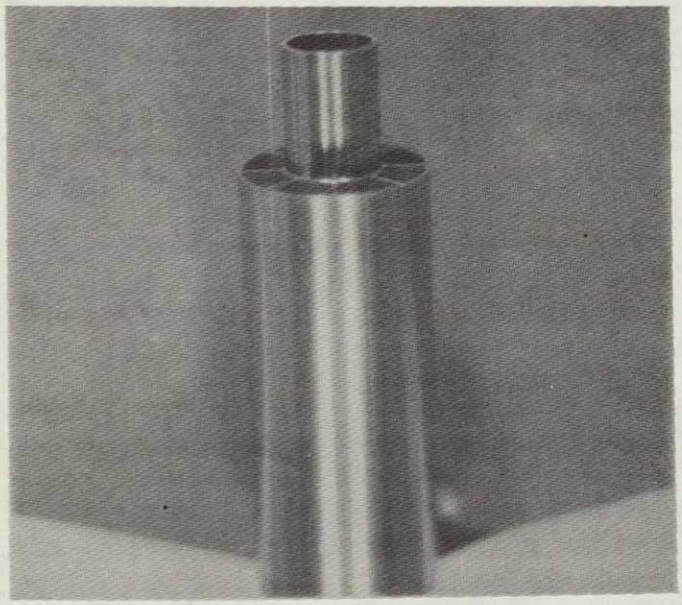

Figure 20. Two Views of Arc-Cast Tungsten Fueled Emitter Structures.

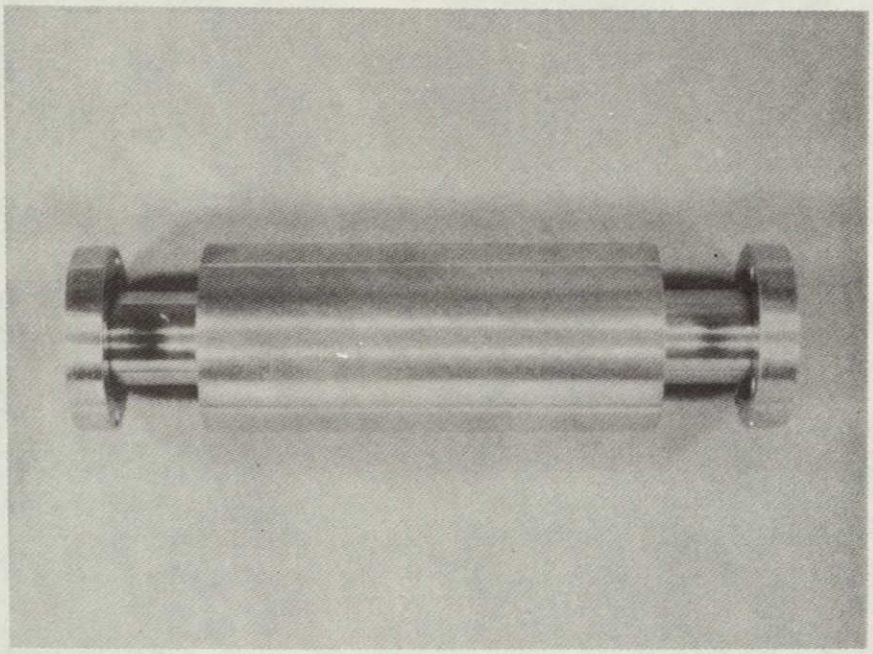

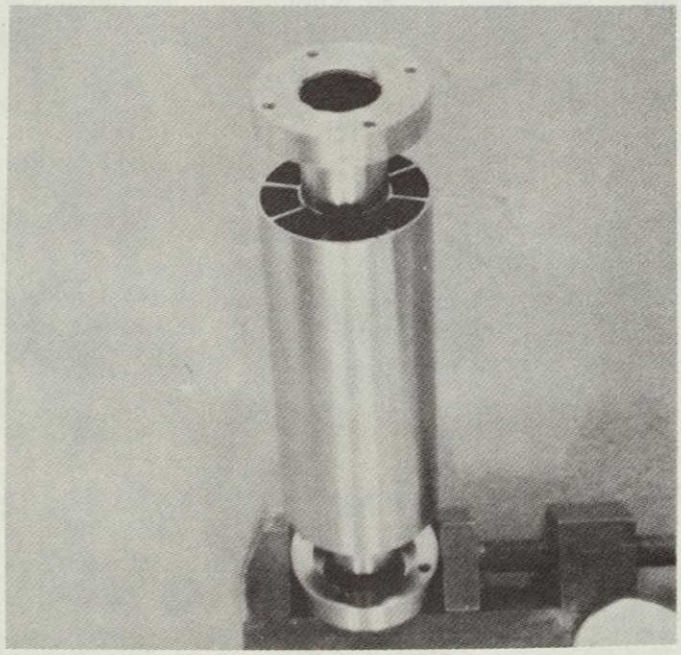

Figure 21. Two Views of Arc-Cast Tungsten Emitter Structure with Niobium End Flanges.

Each of the three emitters was subjected to the following processing and testing schedule

a Place appropriate identification marks
b Hydrogen fire - 900°C for 20 minutes
c Leak check entire part
d Zyglo entire part and inspect for cracks
e Map part dimensionally
f Weld on end flanges
g Leak-check
h Wrap on radiation shields
i Set up for testing
j Thermal cycle
k Remove from test stand
l Leak-check
m Map dimensions
n Zyglo

From the fabrication, processing, and testing schedule, the following items were to be determined

a Does any one fabrication technique lend itself to construction of a full length emitter structure?

b Does thermal cycling the emitter structures cause fracture of the bonds between the webs and the cylinders?

c Does thermal cycling the emitter structure cause dimensional changes?

d Do the emitter structures remain vacuum tight after thermal cycling?

The required thermal condition on the emitter structures was as follows

a Normal emitter temperature 1760°C (2033°K)

b Normal outer fuel enclosure temperature 1869°C (2142°K)

c Heating and cooling rate 20-40°C/minute

d At least 6 thermal cycles

In order to achieve the above condition, the emitters were set up as shown schematically in Figure 22 Thermal calculations show that in order to achieve the 109°C temperature gradient through the tungsten webs, which is equivalent to an emitter heat flux of 50 watts/cm^2 for internal heat generation, an emitter heat flux of 22 watts/cm^2 is required when obtained by externally heating the tungsten outer fuel container The required 22 watts/cm^2 is just about the amount which the tungsten emitter surface can radiate to a cold black-body heat sink Thus, a simple black-body (Cr_2O_3 coated stainless steel) water-cooled tubing inside of the emitter was sufficient to remove the necessary thermal flux

The temperatures of the outer fuel container were observed at three places, and the temperature of the emitter was observed

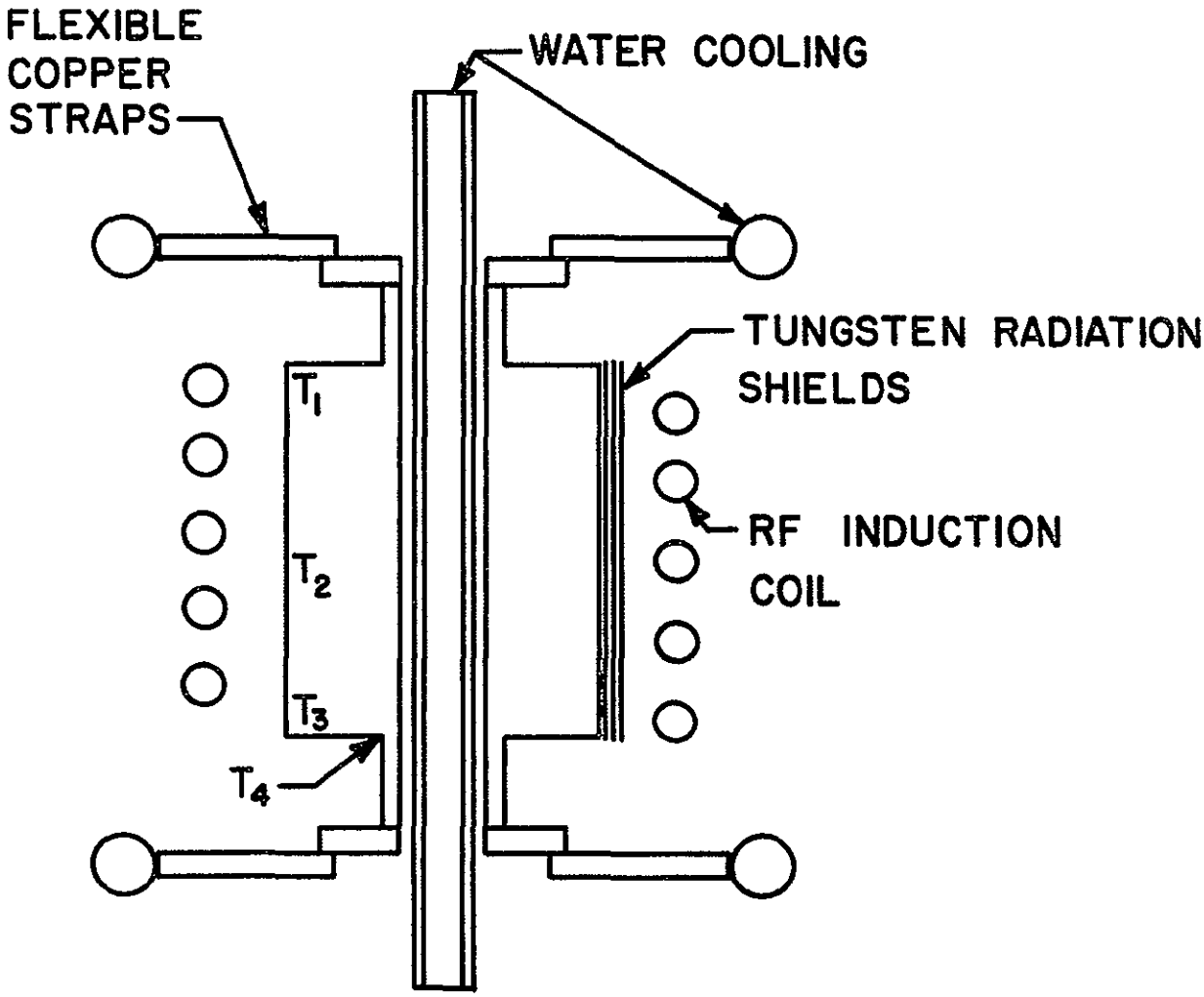

Figure 22 Thermal Cycle Test Setup

at one place (Figure 22) These measurements were made by an optical pyrometer corrected for the bell jar and surface effects The thermal heat flux removed by the central water cooling, determined by calorimetric means, was used as a means of determining the temperature gradient through the webs Since the surface area of the emitter is 33 cm^2, the 22 watts/cm^2 requires 726 watts total to be equivalent to the 109°C temperature gradient through the webs

Each emitter was thermally cycled six times The recorded thermal data are seen in Table II, and the recorded dimensional data are seen in Table III The following can be said about each emitter.

A VACUUM ARC-CAST TUNGSTEN

This emitter was electrical discharge machined from a solid billet of arc-cast tungsten This machining technique does not lend itself to fabricating a full length emitter (10 inches) as the webs have an average taper of 001 inch, over 10 inches, this taper would amount to 0 010 inch out of the desired 0 030 inch thick webs The maximum observed taper was 0 0025 inch/inch, and the minimum observed taper was 0 0003 inch/inch The entire structure was vacuum tight, and remained so throughout thermal cycling, the only exception was the niobium end flanges-to-tungsten welds, which cracked There was no observed change in the emitter inner diameter or in the overall

TABLE II

THERMAL CYCLE TEST DATA

	Cycle #	Time in Minutes			Temperature °C					Heat Watts	$\Delta T(\Omega)$ °C
		Heating	Cooling	At Temp	T_1	T_2	T_3	T_4	AT_w		
Vac Arc Cast Tungsten	1	80	60	30	1759	1892	1708	1613	95	650	98
	2	65	65	90	1767	1887	1720	1613	107	700	104
	3	65	65	120	1826	1928	1772	1654	118	580	86
	4	65	65	165	1805	1915	1750	1650	100	620	92
	5a	70	-	30	1770	1890	1725	1650	75	700	104
	b	-	-	30	1895	1995	1825	1715	110	770	116
	c	-	-	60	1770	1890	1725	1650	75	700	104
	d	-	2	30	1895	1995	1825	1715	110	770	116
	6	60	60	240	1775	1880	1725	1630	95	650	98
CVD Tungsten	1	45	45	90	1920	1880	1790	-	-	925	137
	2	60	60	345	1880	1880	1805	-	-	840	125
	3	60	60	120	1850	1870	1820	-	-	-	-
	4	60	45	75	1905	1945	1825	-	-	700	105
	5	90	50	100	1860	1880	1830	-	-	840	125
	6	70	60	30	1880	1880	1825	-	-	845	125
Hybrid Tungsten	1	45	60	90	1830	1890	1820	1700	120	800	119
	2	90	90	75	1850	1910	1840	1725	115	840	125
	3	60	45	45	1810	1865	1810	1670	140	780	116
	4	45	75	45	1840	1865	1830	1700	130	775	116
	5a	60		15	1810	1865	1820	1710	110	770	116
	b		5	30	1970	1985	1935	1800	135	940	139
	6	45	45	45	1810	1865	1815	1700	115	760	115

TABLE III

EMITTER DIMENSIONAL DATA

	Web - Space	Initial Diameter	Top				Middle				Bottom				Length	
			Final Diameter	Web Change	Space Change	Net Change	Final Diameter	Web Change	Space Change	Net Change	Final Diameter	Web Change	Space Change	Net Change	Before	After
Vac Arc Cast	1	1 2715	1 2713	- 0002		0004	1 2715	0000		0006	1 2712	- 0003		0005	3,0000	3,0001
	1		1 2717		+ 0002	0004	1 2721		+ 0006	0006	1 2717		+ 0002	0005		
	2		1 2713	- 0002		0007	1 2715	0000		0006	1 2712	- 0003		0008		
	2		1 2720		+ 0005	0006	1 2721		+ 0006	0007	1 2720		+ 0005	0008		
	3		1 2714	- 0001		0007	1 2716	+ 0001		0008	1 2712	- 0003		0007		
	3		1 2721		+ 0006	0007	1 2722		+ 0007	0007	1 2719		+ 0004	0006		
	4		1 2714	- 0001		0005	1 2715	+ 0000		0006	1 2713	- 0002		0005		
	4	1 2715	1 2719		+ 0004	0006	1 2721		+ 0006	0006	1 2718		+ 0003	0006		
	Average			- 0002	+ 0004	0006		0000	+ 0006	0006		- 0003	+ 0003	0006		
CVD Tungsten	1	1 2710	—	—			1 2711	+ 0001		0009	1 2713	+ 0003		0006	2,9992	3,0004
	1		—		—		1 2720		+ 0010	0008	1 2719		+ 0009	0012		
	2		1 2710	0000		0006	1 2712	+ 0002		0006	1 2707	- 000		0007		
	2		1 2716		+ 0006	0003	1 2718		+ 0008	0007	1 2714		+ 0004	0006		
	3		1 2713	+ 0003		0005	1 2711	+ 0001		000	1 2708	0002		0008		
	3		—		—		1 2716		+ 0006	0005	1 2716		+ 0006	0009		
	4		—	—			1 2711	+ 0001		0005	1 2707	- 0003		0007		
	4	1 2710	1 2718		+ 0008	0008	1 2716		+ 0006	0005	1 2714		+ 0004	0001		
	Average			+ 0001	+ 0007	0006		+ 0001	+ 0007	0006		- 0001	+ 0006	0007		
Hybrid Tungsten	1	1 2698	1 2700	+ 0002		0008	1 2701	+ 0003		0004	1 2702	+ 0005		0006	3,0002	3 0017
	1	1 2695	1 2705		+ 001	0002	1 2702		+ 0007	0003	1 2694		- 0001	0000		
	2	1 2698	1 2706	+ 0008		0000	1 2702	+ 0004		0008	1 2697	- 0001		0005		
	2	1 2695	1 2703		+ 0008	0007	1 2707		+ 0012	0008	1 2699		+ 0004	0003		
	3	1 2698	1 2699	+ 0001		0010	1 2702	+ 0004		0011	1 2705	+ 0007		0001		
	3	1 2695	1 2706		+ 0011	0010	1 2710		+ 0015	0012	1 2703		+ 0008	0008		
	4	1 2698	1 2699	+ 0001		0007	1 2701	+ 0003		0005	1 2698	+ 0000		0013		
	4	1 2695	1 2703		+ 0008	0006	1 2693		+ 0002	0005	1 2708		+ 0013	0008		
				+ 0003	+ 0009	0006		+ 0003	+ 0008	0007		+ 0003	+ 0006	0005		

length The observed changes in the outer fuel container were an average inward movement of 0002 inch at the webs and an average outward movement between the webs of 0004 inch Thus, the net movement of the outer fuel container was 0006 inch on the diameter, which is comparable to the 3 4 to 4 1 x 10^{-4} inches on a radius predicted by the stress analysis

B CVD FLUORIDE TUNGSTEN EMITTER

This emitter was fabricated by the CVD process on the inner and outer diameter The webs were machined from arc-cast tungsten sheet This fabrication technique appears to be best suited for fabrication of a 10-inch long emitter Ideally, the webs could also be made from CVD fluoride The emitter structure remained vacuum tight throughout the thermal cycling One niobium end flange was welded to the emitter, which was initially vacuum tight but cracked as a result of thermal cycling The other niobium flange was attached by melting the niobium onto the tungsten, without actually alloying the two metals This joint remained vacuum tight throughout the thermal cycles

The dimensional changes which occurred were different from in the first emitter The entire emitter swelled on the outer diameter (by an average of 0001 inch) and length (by an average of 0012 inch) Swelling of CVD fluoride tungsten has been observed by Thermo Electron in previous tests in connection with the GGA and GE TFE development The net charge in the outer fuel container between the webs and the spacer was 0 0006 inch on a diameter, which is the

same amount as the first emitter Comparing this emitter to the first emitter indicates that the gross swelling was 0004 inch on the diameter rather than the measured 0001 inch The dimensional change on the inner diameter could not be checked due to some alloying of the central cooling tube with the emitter, which occurred when a seventh thermal cycle was attempted without water in the central tube

C HYBRID TUNGSTEN EMITTER

The inner cylinders and webs of this emitter were fabricated from arc-cast tungsten The outer cylinder was CVD fluoride tungsten The technique for fabricating the webs and inner cylinder was identical to that used in fabricating the first all arc-cast tungsten emitter Accordingly, the webs are tapered up to a total of 0 006 inch in the 030 inch thickness If a full length emitter was to be made by this method, the tapered webs could be alleviated by electrical discharge machining from the outer diameter inward rather than from one end to the other, however, this would not necessarily solve all problems, as the free standing webs would be highly stressed during machining

Another problem associated with the fabrication of emitters from all or partially arc-cast tungsten is that of cracking of the tungsten An example of this is seen in Figure 23, which is an end view of the hybrid emitter This emitter was cracked in several places on the inner cylinder and webs Even though this emitter was cracked, it was thermally cycled in order to obtain a cross sectional view of the CVD outer cylinder joint to the webs, and the niobium flange melt to the tungsten sleeve

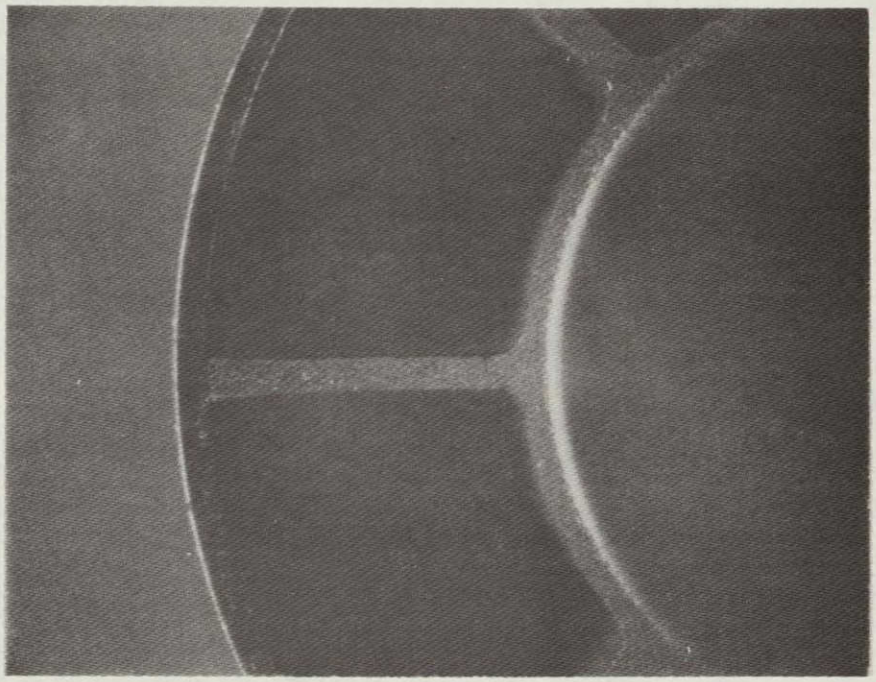

Figure 23. End View of Hybrid Emitter.

The thermal cycling of this emitter produced results similar to those seen when cycling the all CVD emitter. The entire emitter grew in outer diameter by 0.0003 inch and the length grew by 0.0015 inch. The net change in the outer fuel container from the webs to the midpoint between the webs was 0.0006 inch.

A cross sectional view of the emitter is seen in Figure 24. Figure 25 shows a typical web-to-outer fuel container joint and Figure 26 shows a typical view of the CVD fluoride outer fuel container. There were no observed differences in the CVD outer fuel container around the diameter and along the length. Also, there was no observed coalescing of fluorine into bubbles along the grain boundaries, as is sometimes prevalent in high fluoride content CVD tungsten.

Figure 27 shows the niobium melt-to-tungsten joint. As can be seen from the photographs, there was no alloying, but there was a good braze made.

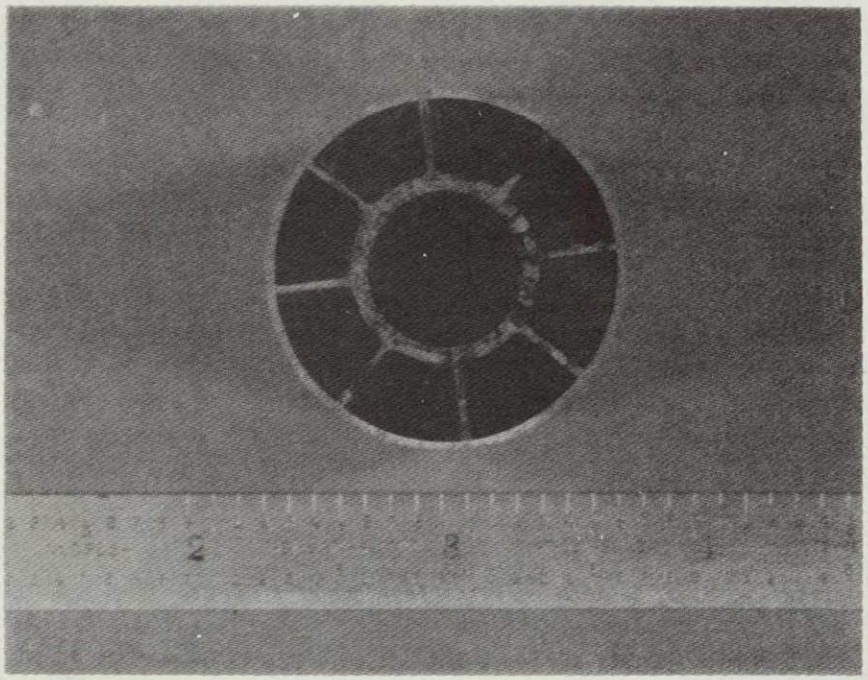

Figure 24. Cross Sectional View of Hybrid Emitter.

CVD →

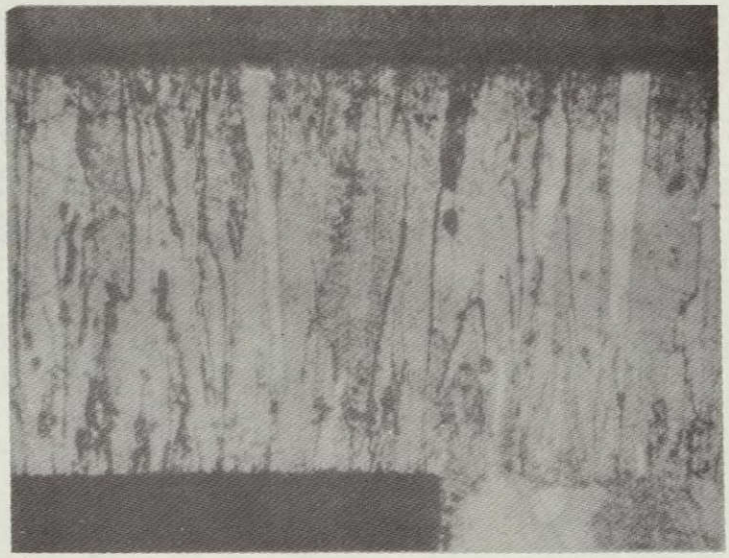

CVD→

VAC→

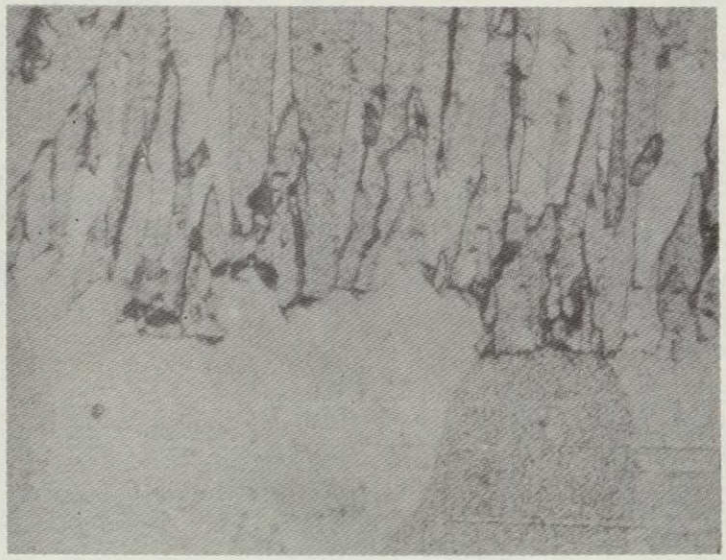

(280x)

Figure 25. CVD-to-VAC Web Joint.

Machined outside

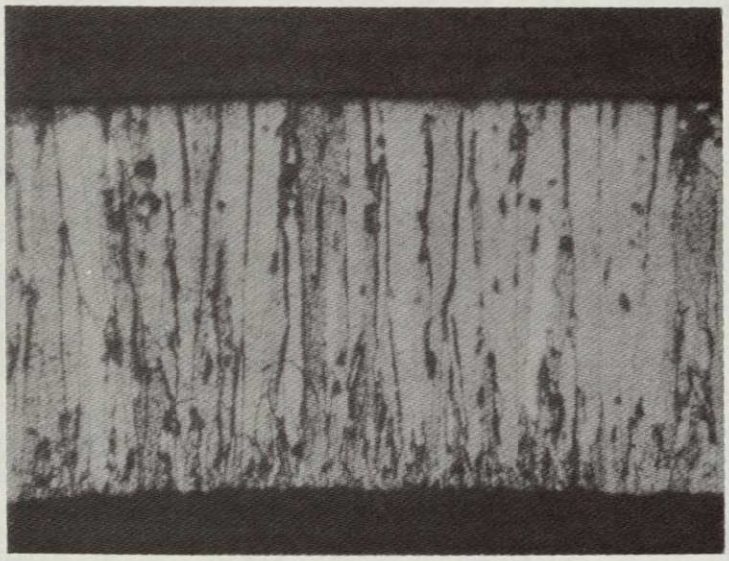

As-deposited inside

Figure 26. CVD Fluoride Tungsten.

W Nb

(70x)

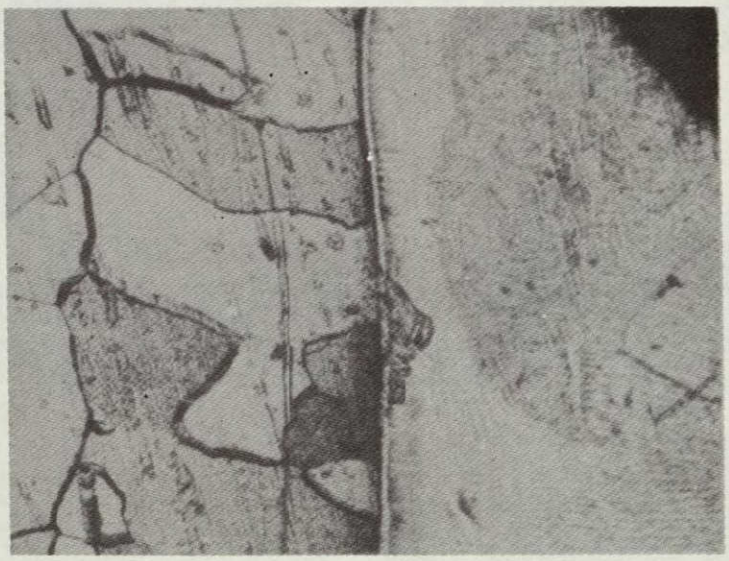

W Nb

(140x)

Figure 27. Niobium-to-Tungsten Melt Braze.

VII CONCLUSIONS AND RECOMMENDATIONS

From the fabrication and thermal cycling of the three different emitters, the following conclusions can be drawn

a The all-CVD fluoride tungsten emitter lends itself to the fabrication of a full length (10 inch) emitter

b Thermal cycling of the emitter does not cause fracture of the webs or of the joints between the webs and the inner and outer cylinders

c Thermal cycling of the emitter does cause some permanent deformation of the outer fuel container, however, it is within the predicted range and is not detrimental to the operation of the emitter structure

In order to investigate the all-bonded emitter structure fully, it is recommended that an all-CVD fluoride tungsten emitter (including webs) be fabricated and that representative end caps be welded in place over the fuel location This structure should be thermally cycled to determine the effects of the end closures

After successful completion of a three-emitter thermal test, it is recommended that a full-length, 10-inch emitter be fabricated and tested After successful completion of a full-length emitter test, it is further recommended that a fueled full-length diode be fabricated employing an all-CVD fluoride tungsten emitter

VIII REFERENCES

1 J Dunlay and R Meyers, "Sublimed Coatings for Emitter and Collector Surfaces," 1970 Thermionic Conversion Specialists Conference, October 1970, Miami, Florida

2 Donald M Ernst, "Thermionic Performance of CVD Chloride Tungsten and Sublimted Coated Molybdenum Electrodes in Cylindrical Heat Pipe Diodes, " 1970 Thermionic Conversion Specialists Conference, October 1970, Miami, Florida

3 R Roark, Formulas for Stress and Strain, New York McGraw Hill Book Company, Inc , 1954

4 Z Zudens, T C Yen and W H Steigelmann, Thermal Stress Techniques in the Nuclear Industry, New York American Elsevier Publishing Company, Inc , 1965

5 S Kitrilakis and M Meeker, Advanced Energy Conversion, Volume 3, pp 59-68 (1963)

APPENDIX A

DIODE PERFORMANCE CALCULATION

Figure A-1 is an extrapolated J-V curve at an emitter temperature of 2000°C for the proposed active electrode surfaces [1,2] From this curve, the electrode power density is seen to be 8 27 watts/cm^2 (1 15 volts at 7 2 amps/cm^2) In order to reduce this to the diode terminal efficiency, the internal resistive losses must be subtracted These losses are determined in the following manner

Since the diode is double-ended, half the current flows through half the length of the emitter-collector pair and down one emitter and collector sleeve Therefore,

I = Total diode current (sum of two ends)
R_E = Total emitter resistance
R_C = Total collector resistance
R_{ES} = Emitter sleeve resistance (one end)
R_{cs} = Collector sleeve resistance (one end)
P_L = Total power loss

Now

$$P_L = \Sigma I^2 R$$

Thus,

$$P_L = 2\int_0^{\frac{L}{2}} (JA_E)^2 \frac{\rho_E dL}{A_{EC}} + (JA_E)^2 \frac{\rho_C dL}{A_{CC}} + 2(\frac{I}{2})^2 (R_{ES} + R_{CS})$$

where

J = Emitter current density, A/cm^2
A_E = Surface area of emitter, cm^2
ρ_E = Resistivity of emitter, Ω-cm
L = Total length of emitter or collector, cm

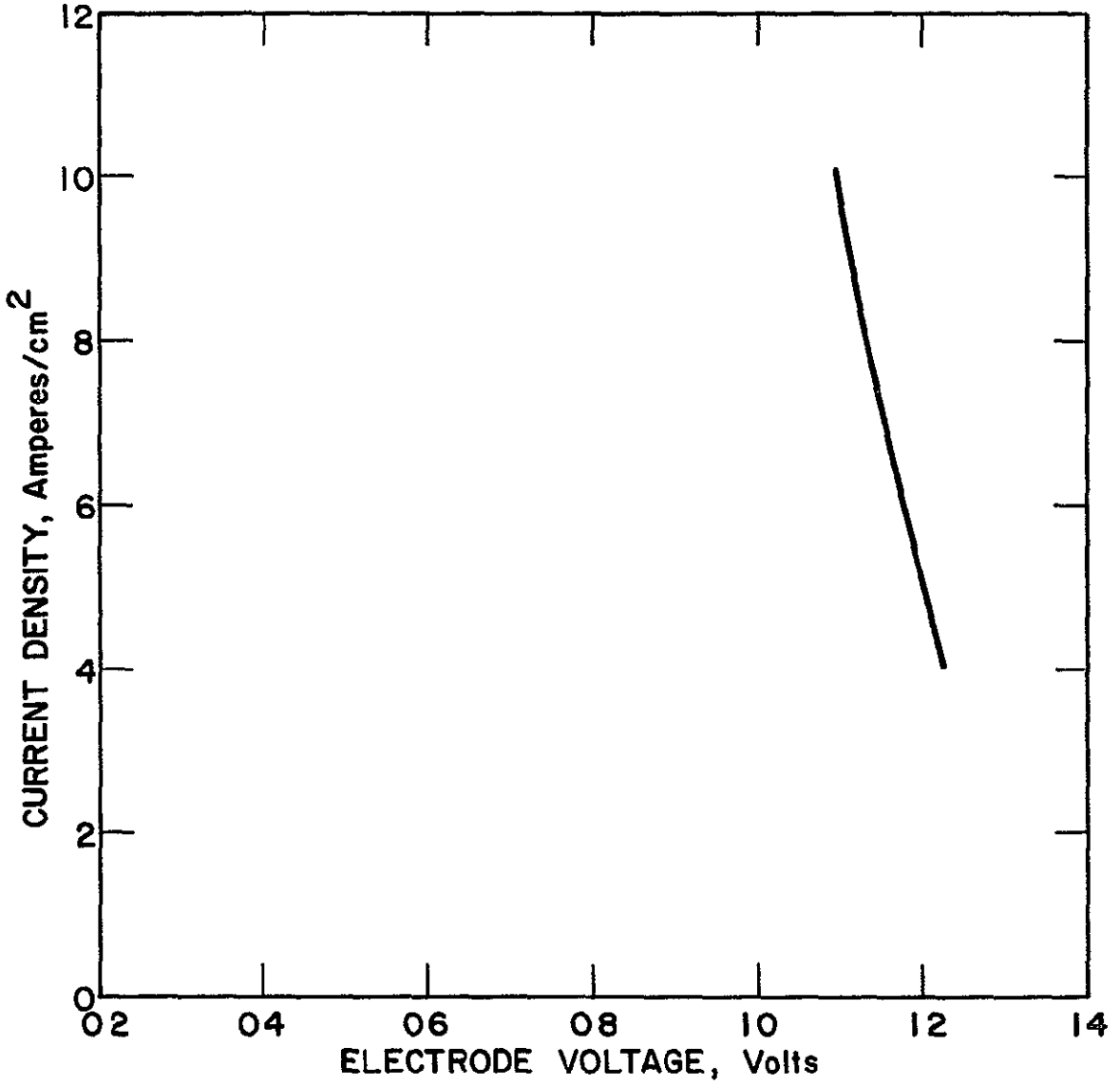

Figure A-1 Thermionic Performance of Proposed Active Electrodes

A_{EC} = Emitter cross sectional area, cm^2

ρ_C = Resistivity of collector, Ω-cm

A_{CC} = Collector cross sectional area, cm^2

Now,

$$P_L = \int_0^{\frac{L}{2}} (J\pi DL)^2 \left(\frac{\rho_E}{A_{EC}} + \frac{\rho_C}{A_{CC}}\right) dL + 2\left(\frac{I}{2}\right)^2 (R_{ES} + R_{CS})$$

where

D = Emitter diameter

Integrating, we have

$$P_L = 2J^2\pi^2 D^2 \left(\frac{\rho_E}{A_{EC}} + \frac{\rho_C}{A_{CC}}\right) \frac{L^3}{3} \Bigg|_0^{\frac{L}{2}} + \frac{2I^2}{4} (R_{ES} + R_{CS})$$

Collecting terms, we have

$$P_L = \frac{I^2}{12} (R_E + R_C) + \frac{I^2}{2} (R_{ES} + R_{CS}),$$

which are the total resistive losses within the diode in terms of the total current, total resistance of the emitter and collector, and the resistance of the emitter and collector sleeves

The surface area of the emitter is

$$A_E = \pi D l = 3\ 14\ (\ 550)(2\ 54)(10)(2\ 54) = 111\ Cm^2$$

The resistance of the emitter is

$$R_E = \frac{\rho_E L}{A_{EC}} = \frac{\rho_e L}{\pi (r_2^2 - r_1^2) + 16\ (\ell t)} ,$$

where ℓ = width of web,

t = thickness of web,

$$R_E = \frac{56 \times 10^{-6} \times 10 \times 2\ 54}{3\ 14(2\ 54)^2\ [\ 335^2 - \ 275^2\ ] + 16(\ 290)(\ 03)(2\ 54)}$$

$$= 8\ 65 \times 10^{-4} \text{ ohms}$$

The resistance of the collector is

$$R_L = \frac{\rho_C L}{A_{CC}} = \frac{\rho_c L}{\pi(r_2^2 - r_1^2)}$$

$$= \frac{42 \times 10^{-6} \times 10 \times 2\ 54}{3\ 14(\ 275^2 - \ 15^2)(2\ 54)^2}$$

$$= 9\ 9 \times 10^{-4} \text{ ohms}$$

The resistance of the emitter sleeve is

$$R_{ES} = \frac{\bar{\rho} L}{A} = \frac{\rho\ L_s}{\pi(r_2^2 - r_1^2)}$$

$$= \frac{40 \times 10^{-6}(\ 8)(2\ 54)}{3\ 14(\ 315^2 - 275^2)(2\ 54)^2}$$

$$= 1\ 71 \times 10^{-4} \text{ ohms}$$

The resistance of the collector sleeve is

$$R_{CS} = \frac{\rho\ L_C}{A_{CC}}$$

$$= \frac{40 \times 10^{-6}(1\ 25)(2\ 54)}{3\ 14(\ 275^2 - \ 15^2)(2\ 54)^2}$$

$$= 1\ 24 \times 10^{-4} \text{ ohm}$$

Using Equation A-1, we have

$$P_L = \frac{(7\ 2 \times 111)^2}{12} [8\ 65 \times 10^{-4} + 9\ 9 \times 10^{-4}] + \frac{(7\ 2 \times 111)^2}{2}$$

$$[1\ 71 \times 10^{-4} + 1\ 24 \times 10^{-4}]$$

P_L = 194 watts, which is 1 75 watts/cm^2 of emitter area

Thus, the terminal power density is the electrode power density minus the resistive losses

$$P_T = P_e - P_L$$

$$= 8\ 27 - 1\ 75$$

$$= 6\ 52 \text{ watts/cm}^2$$

Now the total power input is a sum of the heat loss from the emitter, which is

$$P_{IN} = \Sigma P_{1-6}$$

P_1 = Radiation from the emitter to collector
P_2 = Radiation from the fuel enclosure
P_3 = Conduction down the emitter sleeve
P_4 = Conduction down the fuel enclosure
P_5 = Cesium conduction
P_6 = Electron cooling

$$P_1 = 5\ 67 \times 10^{-12} \epsilon_{eff} A_E (T_2^4 - T_1^4),$$

where

ϵ_{eff} = Effective emissivity = 0 2 (measured)
A_E = 111 cm^2
T_2 = 2000°K
T_1 = 1000°K
P_1 = 1900 watts = 17 11 watts/cm^2
P_2 = 5 67 x 10^{-12} $\epsilon_{eff} A_{FE} (T_2^4 - T_1^4)$

Assuming the entire end of the diode (1 30 inches in diameter) radiates from 2000°K to 1000°K with ϵ_{eff} = 0 2, then,

$2 A_{FE}$ = $2\pi (2 = 2 \times 3\ 14\ (2\ 54)^2\ (\ 65)^2$ = 17 1 cm^2

P_2 = 243 watts = 2 57 watts/cm^2

P_3 = $2 \left(\frac{K A \Delta T}{L} \right)$,

where

K = Mean thermal conductivity of emitter sleeve
ΔT = Temperature gradient on sleeve
L = Length of section
A = Cross sectional area of sleeve

$$P_3 = \frac{2\ (1\ 04)\ (3\ 14)\ (2\ 54)^2\ (\ 315^2 - \ 275^2)\ (1000)}{8\ (2\ 54)}$$

= 486 watts
= 4 38 watts/cm^2

The conduction losses down the fuel enclosure will be approximated at 1/4 of those down the emitter sleeve Thus,

P_4 = 142 watts = 1 1 watts/cm^2

The cesium conduction will be taken as the maximum which occurs in a 0 010 inch spacing diode [5]

$$P_5 = 2\ 5 \text{ watts/cm}^2$$

The electron cooling is taken as $J\phi_e$, where ϕ_e is the Richardson work function for the cesiated emitter

$$P_6 = \phi_e J$$
$$= 3\ 110\ (7\ 2)$$
$$= 22\ 4 \text{ watts/cm}^2$$

Thus, the total power input to the emitter is.

$$P_{IN} = 17\ 11 + 2\ 57 + 4\ 38 + 1\ 1 + 2\ 5 + 22\ 4$$

$$P_{IN} = 50.06 \text{ watts/cm}^2$$

Now the efficiency $= \frac{P_o}{P_{in}} = \frac{6\ 52}{50\ 06} = 13\%$

$$\eta = 13\%$$